Proton NMR of *Escherichia coli* Sulfite Reductase: The Unligated Hemeprotein Subunit†

Jeffrey Kaufman,‡ Leonard D. Spicer,*,‡,§ and Lewis M. Siegel*,‡

Departments of Biochemistry and Radiology, Duke University Medical Center, Durham, North Carolina 27710

Received August 26, 1992; Revised Manuscript Received December 21, 1992

ABSTRACT: The isolated hemeprotein subunit of sulfite reductase (SiR-HP) from *Escherichia coli* consists of a high spin ferric isobacteriochlorin (siroheme) coupled to a diamagnetic $[4Fe\text{-}4S]^{2+}$ cluster. When supplied with an artificial electron donor, such as methyl viologen cation radical, SiR-HP can catalyze the six electron reductions of sulfite to sulfide and nitrite to ammonia. Thus, the hemeprotein subunit appears to represent the minimal protein structure required for multielectron reductase activity. Proton magnetic resonance spectra are reported for the first time on unligated SiR-HP at 300 MHz in all three redox states. The NMR spectrum of high spin ferric siroheme at pH 6.0 was obtained for the purpose of comparing its spectrum with that of oxidized SiR-HP. On the basis of line widths, T_1 measurements, and 1D NOE experiments, preliminary assignments have been made for the oxidized enzyme in solution. The pH profile of oxidized SiR-HP is unusual in that a single resonance shows a 9 ppm shift over a range of only 3 pH units with an apparent $pK = 6.7 \pm 0.2$. Resonances arising from the β-CH_2 protons of cluster cysteines have been assigned using deuterium substitution for all redox states. One β-CH_2 resonance has been tentatively assigned to the bridging cysteine on the basis of chemical shift, T_1, line width, and the presence of NOEs to protons from the siroheme ring. The observed pattern of hyperfine shifts can be used as a probe to measure the degree of coupling between siroheme and cluster in solution. The cluster iron sites of the resting (oxidized) enzyme are found to possess both positive and negative spin density which is in good agreement with Mossbauer results on frozen enzyme. The NMR spectrum of the 1-electron reduced form of SiR-HP is consistent with an intermediate spin ($S = 1$) siroheme. Intermediate spin Fe(II) hemes have only been previously observed in 4-coordinate model compounds. However, the amount of electron density transferred to the cluster, as measured by the isotropic shift of β-CH_2 resonances, is comparable to that present in the fully oxidized enzyme despite diminution of the total amount of unpaired spin density available. Addition of a second electron to SiR-HP, besides generating a reduced $S = 1/2$ cluster with both upfield and downfield shifted cysteine resonances, converts siroheme to the high spin ($S = 2$) ferrous state. The large magnitude of the hyperfine shifts observed for the β-CH_2s of cluster cysteines in all three redox states studied requires that exchange coupling between the heme and the cluster be maintained in solution in all redox states of unligated SiR-HP.

NADPH–sulfite reductase of *Escherichia coli* is a multimeric ($\alpha_8\beta_4$) hemoflavoprotein ($M_r = 685\,000$) which catalyzes the six electron reductions of SO_3^{2-} to S^{2-} and NO_2^- to NH_3 (Siegel et al., 1973, 1979; Siegel & Davis, 1974). This enzyme's physiological role, as shown by genetic studies (Kemp et al., 1963), is the provision of reduced sulfur for biosynthesis; therefore the *E. coli* enzyme is an "assimilatory" type sulfite reductase. A second enzyme class, the "dissimilatory" sulfite reductases, are involved in the use of sulfite as a terminal electron acceptor in certain anaerobic bacteria (Peck & Lissolo, 1988). The *E. coli* hemoflavoprotein complex can be dissociated in 3–4 M urea into an α_8-octamer and 4 β-monomers (Siegel & Davis, 1974). The β-subunit, $M_r = 64\,000$ (Ostrowski et al., 1989), contains two prosthetic groups, a siroheme (an Fe–isobacteriochlorin; Murphy et al., 1973; Scott et al., 1979; see Figure 1) and an iron–sulfur cluster of the [4Fe-4S] type (Christner et al., 1983b). The SiR[1] hemeprotein monomer cannot use NADPH as an electron donor for sulfite reduction, since the flavin components are missing; it can, however, use other electron donors such as methyl viologen cation radical. Interaction of the two prosthetic groups may be of functional significance in facilitating the rapid transfer of multiple reducing equivalents to the bound substrate (Siegel

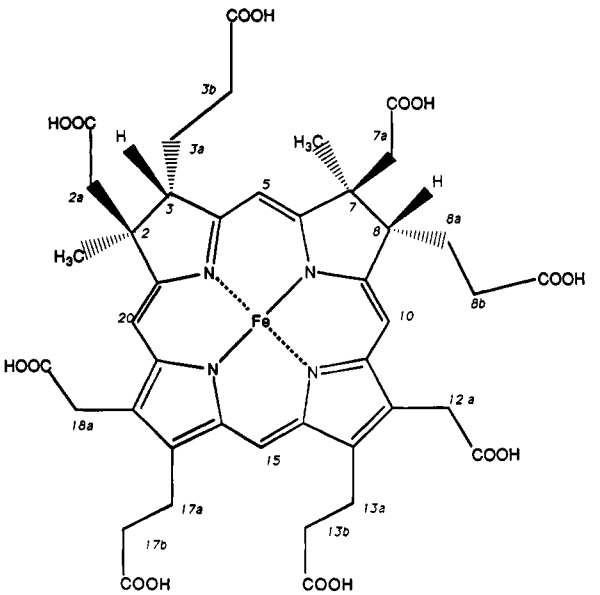

FIGURE 1: Structure of siroheme showing the labeling scheme used.

† This research was supported in part by Veterans Administration Project Grant 215406554-01 to L.M.S. and National Institutes of Health Grants R01GM41829 (to L.D.S.) and R01GM21226 (to L.M.S.).

* Authors to whom correspondence should be addressed.

‡ Department of Biochemistry.

§ Department of Radiology.

0006-2960/93/0432-2853$04.00/0

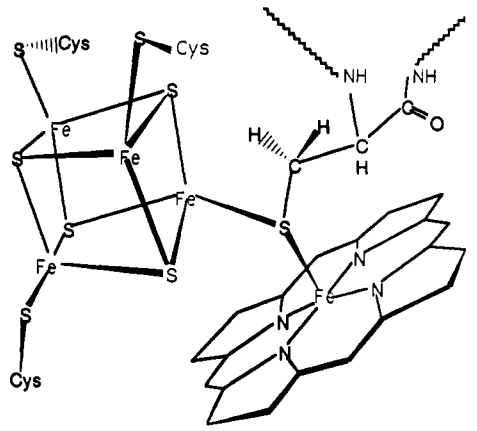

FIGURE 2: Model of the active site in *E. coli* sulfite reductase hemeprotein subunit showing a bridging cysteinyl sulfur between the cluster and the heme.

& Wilkerson, 1989). The existence of a chemical linkage between the siroheme and the cluster is strikingly manifested in the form of magnetic exchange coupling between the two prosthetic groups, which on the basis of Mossbauer (Christner et al., 1981; 1983a,b, 1984), ENDOR (Cline et al., 1985, 1986), and EPR spectroscopy (Janick & Siegel, 1982, 1983) has been shown in frozen samples to persist in various redox states of the enzyme, in both the presence and absence of exogenous ligands. A model of the active site has been proposed (Janick & Siegel, 1982; see Figure 2) in which one cluster Fe is covalently bridged to the siroheme Fe by the sulfur of a cysteinyl cluster ligand. X-ray crystallographic data at 2.8 Å resolution (McRee et al., 1986) are consistent with this model, although the preliminary structure of the active site of SiR-HP obtained from these data lacks sufficient resolution to identify the bridging ligand. Resonance Raman data suggest that a sulfur atom bridges the heme Fe to the [4Fe-4S] cluster (Madden et al., 1989). The preliminary crystallographic evidence also indicates that the edge of the siroheme macrocycle appears to be in Van der Waals contact with a cubane S atom of the cluster. This may present another means by which the π orbitals of siroheme can interact with the cluster.

The goal of this work is to use paramagnetic NMR to characterize all three redox states of the unligated enzyme in solution. In the presence of a paramagnetic center, hyperfine shifted resonances can be observed outside the normal diamagnetic envelope and so act as a probe of the active site in proteins too large to study by more traditional NMR techniques. Metalloproteins that have been successfully studied by paramagnetic NMR include both heme and iron–sulfur containing enzymes. Recently, the first report appeared in the literature (Cowan & Sola, 1990) of ^{1}H NMR on assimilatory sulfite reductase from *Desulfovibrio vulgaris* (Hildenborough). This enzyme also contains a siroheme and [4Fe-4S] cluster, although, unlike the *E. coli* enzyme, it has a low spin ferric siroheme. Tan and Cowan (1991) have postulated that it contains sulfide rather than cysteine as the bridging ligand. Their spectroscopic data are also consistent, however, with sulfide as the sixth ligand to the heme, rather than the bridging ligand.

If the protons on chromophores and residues ligating the paramagnetic center can be assigned, they can be subsequently used to identify the magnetic and electronic properties of prosthetic groups or used to identify neighboring ionizable residues by pH titration. We report here the unambiguous assignment of the cluster cysteine β-CH_2s in *E. coli* SiR-HP utilizing deuterium substitution. Evidence is presented to tentatively identify one of the β-CH_2 protons as belonging to the bridging ligand, providing support for the cysteine-bridged model of the active site of SiR-HP in solution. We demonstrate the presence of an intermediate $S = 1$ ferrous heme which remains coupled to the cluster in SiR-HP^{1-}. We suggest how the isotropic shift of cluster cysteines may be used as a probe to measure spin density transfer from the heme to the cluster and hence to measure coupling, and evidence is presented that in solution a bridge between cluster and siroheme is maintained for all redox states of unligated SiR-HP. pH titration of resting SiR suggests that an ionizable amino acid group is near the heme. Lastly, we confirm the results of previous resonance Raman data (Han et al., 1989a) that siroheme in the fully reduced state is $S = 2$ and report the first NMR spectrum for isolated siroheme.

MATERIALS AND METHODS

E. coli K12 was grown in bulk (90–100 kg) on minimal media (Siegel et al., 1973; Grain Processing Corp., Muscatine, IA) and stored at 2.5-kg cakes at 77 K until used. *E. coli* NADPH–sulfite reductase was purified from this cell paste by published procedures (Siegel et al., 1973; Siegel & Davis, 1974) with the following minor modifications: The final agarose column step was omitted. The hemeprotein subunit was dissociated from the holoenzyme present after the second ammonium sulfate precipitation step by room temperature incubation in 3 M urea–10 mM KP_i (pH 7.7) for 30 min followed by DEAE-cellulose chromatography in 50 mM KP_i–4 M urea–100 μM EDTA (pH 7.7). The SiR-HP was further purified by application to a column of phenyl-Sepharose CL4B (Pharmacia) equilibrated in 100 mM KP_i (pH 7.7)–1.0 M ammonium sulfate followed by a step gradient of 0.5, 0.3, and 0.1 M ammonium sulfate in SBE. The isolated SiR-HP was divided into two pools by the purity index (A_{280}/A_{387}). Protein with a purity index less than 1.75 was used for NMR studies while that with an index greater than 1.75 was used solely for heme extraction. In cases where only siroheme was desired, the final column step was omitted. Following isolation and dialysis vs SBE, the protein was concentrated by Amicon filtration to 110 μM and stored in liquid nitrogen until used. Concentrations were determined spectrophotometrically using an $\epsilon_{591} = 18.1$ mM^{-1} cm^{-1} (Siegel et al., 1982).

Later studies used sulfite reductase obtained from plasmid overproducers of the holoenzyme or the hemeprotein subunit. The holoenzyme overproducer consisted of a pT7T3 plasmid with *cys*I, *cys*J, and *cys*G under native promoter control (Wu et al., 1991). The plasmid was grown in a strain of *Salmonella typhimurium* that was *cys*I$^-$ so that only the *E. coli* sulfite reductase was present. Cells were grown on minimal salts media (Medium E; Vogel & Bonner, 1956) at 37 °C in a New Brunswick fermentor with a working volume of 174 L. Typical yields were 500–800 g of wet cell paste per run with 5–15 mg of sulfite reductase holoenzyme/g of cell paste. The isolation procedure for holoenzyme (Siegel et al., 1973) was modified

[1] Abbreviations: SiR, sulfite reductase; SiR-HP, oxidized sulfite reductase hemeprotein subunit; SiR-HP^{1-}, half-reduced SiR-HP; SiR-HP^{2-}, fully-reduced SiR-HP; EDTA, ethylenediaminetetraacetic acid; SB, standard buffer 0.1 M KP_i (pH 7.7); SBE, standard buffer with 100 μM EDTA; EPR, electron paramagnetic resonance; OEiBC, octaethyliso-bacteriochlorin; [4Fe-4S]$^{2+/1+}$, oxidized, reduced four-iron–four-sulfur cluster; NOE, nuclear Overhauser effect; HPLC, high-performance liquid chromatography; HiPiP, high-potential iron–sulfur protein; RR, resonance Raman; OEP, octaethylporphyrin; δ_{con}, contact shift; PEI, poly-ethyleneimine; KP_i, potassium phosphate; DSS, 2,2-dimethyl-2-sila-pentane-5-sulfonate; Dlfl, deazalumiflavin.

Table I: Purification of Sulfite Reductase

step and fraction	*E. coli* WT[b]			SiR-holoenzyme overproducer			SiR-HP overproducer		
	mg of protein	mg[c] of HP	ratio[d]	mg of protein	mg[e] of HP	ratio[d]	mg of protein	mg[f] of HP	ratio[d]
1. crude extract[a]	1000	0.872	0.087	1000	43.7	4.37	1000	18.5	1.85
2. PEI supernatant	790	0.870	0.102	952	40.2	4.22	394	13.1	3.31
3. first $(NH_4)_2SO_4$ precipitate	291	0.750	0.258	887	35.9	4.04			
4. calcium phosphate gel eluant	9.39	0.639	6.81	101	30.3	30.0			
5. second $(NH_4)_2SO_4$ supernatant	na[h]	na	na				349	12.9	3.67
6. second $(NH_4)_2SO_4$ precipitate	2.8	0.515	18.4				161	10.2	6.34
7. post-DE-52					12.12	100.0[g]	24	5.2	21.7
8. post-phenyl-Sepharose column					10.67	100.0[g]	8.2	4.8	58.0
9. post-agarose column	1.48	0.443	30.0[i]						

[a] All data were normalized to an initial crude extract which contains 1000 mg of protein. [b] Data taken from Siegel et al. (1973). Note that protamine sulfate and not PEI was used in this preparation. [c] To calculate the milligrams of hemeprotein present, the NADPH–sulfite reduction assay was used with the specific activity of 2.9 units/mg of holoenzyme (Sigel et al., 1973). [d] The ratio represents the milligrams of hemeprotein present divided by the total protein times 100. [e] To calculate the milligrams of SiR-HP present, the NADPH–hydroxylamine reductase assay was used with the specific activity of 20 units/mg of HP. The initial amount of holoenzyme present was 134 mg/g of protein. [f] Measured optically by using the extinction coefficient of 18.1 mM^{-1} cm^{-1} at 590 nm (Siegel et al., 1982). [g] Based on A_{280}/A_{387} ratio of 1.66 for pure SiR-HP (Siegel et al., 1973). [h] na = data not available. [i] Represents purified holoenzyme with an A_{280}/A_{387} ratio of 3.6 (Siegel et al., 1973). In pure SiR holoenzyme, only 30% of the protein is SiR-HP.

as follows (see Table I): The amount of KCl added to the PEI supernatant was increased to 0.8 M. The amount of aged calcium phosphate gel added was determined by titrating the hydroxylamine reductase activity (Siegel et al., 1973). Calcium phosphate gel was added until the residual activity in the supernatant was less than 10% of the initial activity. After being washed with one volume of SBE/2, the gel was resuspended in three volumes of 0.2 M KP_i (pH 7.7). The SiR holoenzyme showed an optical spectrum that had lower 590 nm and 386 nm absorptions as compared to the 405 nm and 440 nm peaks that have previously been reported for SiR holoenzyme isolated from wild-type *E. coli* (Siegel et al., 1973). Unpublished studies (Wu, Kredich, and Siegel) have shown that this result is due to an excess production of SiR-FP as compared to SiR-HP in the strains used in this work. SiR-FP largely copurifies with holoenzyme through the second ammonium sulfate precipitation step (Ostrowski et al., 1989). SiR-HP was prepared from the holoenzyme by urea dissociation and subsequent DE-52 and phenyl-Sepharose chromatography as described above.

A second overproducing strain grown expressed the hemeprotein subunit under tac promoter control in *E. coli*. The advantage of using this strain is that cells will continue to produce sulfite reductase in the presence of cystine, an inhibitor of the native promoter. Additionally, it was observed that DL-cystine did not inhibit cell growth (as was observed for the *Salmonella* overproducer). This strain was used when cells were grown on DL-cystine-(3,3,3′,3′-d_4). Cultures were grown in 2-L flasks (850 mL/flask) on a shaker table at 37 °C. The minimal medium was supplemented with 0.5 mM DL-cystine and a mixture of amino acids. Growth was monitored optically at 550 nm. Inducer, isopropyl β-D-thiogalactopyranoside (IPTG), was added at an absorbance of 0.7 and the cells were harvested at an absorbance of 2.5. Typical yields were 2–3 g/L of medium with 1–1.5 mg of SiR-HP/g of cell paste present in the crude supernatant after sonification and centrifugation. The purification procedure used is as follows (Table I). All steps were performed at 4 °C. To the crude supernatant was added 10% PEI (86.9 mL/1000 mL of crude), and the mixture was then stirred for 30 min. Next, the solution was brought to 0.8 M in KCl and allowed to stir for an additional 30 min prior to centrifugation. An ammonium sulfate fractionation was performed by adding first 250 g/L, centrifuging, and then adding an additional 150 g/L to the supernatant. Following centrifugation, the second pellet was taken up in a small volume of SBE/2 and dialyzed versus 4 L of SBE/2 two times for 4 h and lastly overnight. Despite the absence of urea, SiR-HP was found to be unstable for long periods of time in 10 mM KP_i (pH 7.7). The protein was dialyzed against 4 L of 10 mM KP_i (pH 7.7) twice for 2 h each time and then placed on the DE-52 column. The sample was washed with 100 mL each of 10 mM and 20 mM KP_i before being eluted with 50 mM KP_i (all at pH 7.7). Lastly, the sample was chromatographed on a phenyl-Sepharose column as previously described. The final SiR-HP product obtained from all overproducers was identical to the native enzyme in regard to specific activity and optical, EPR, and NMR spectra.

HPLC was performed using a Waters 600E system controller, 745 data module, and U6K injector containing a 1-mL loop. Peaks were detected optically by either a Milton Roy spectroMonitor 3100 at 386 nm or a Waters 484 tunable absorbance detector at 254 nm. A C18 Brownlee guard column (3 cm × 4.6 mm ID, 5 μm particles) followed by a Beckman μ-Bondpack C18 (25 cm × 4.6 mm i.d., 5-μm particles) column was used in all purifications. All solvents were HPLC grade from Aldrich. Johnson and Mathey ultrapure acetic acid was used to adjust the pH. The ammonium acetate was Gold Label grade from Aldrich.

EPR spectra were taken with a Bruker ER200D spectrometer at a nominal temperature of 15–20 K, a modulation amplitude of 10 G, an operating frequency of 9.47–9.48 GHz, and a modulation frequency of 100 kHz. Spin concentrations were determined from spectra recorded under nonsaturating conditions either by double integration and comparison with Cu(II)–EDTA standard or by integration of an absorption type peak and comparison with a standard of known concentration. A Hewlett-Packard 9825A computer equipped with 9874A digitizer and 7225A graphics plotter was used for integration and plotting of spectra.

NMR spectra were run in double precision mode over 16K data points on either the General Electric GN-300 MHz spectrometer with a 12-bit ADC or the GN-500 MHz spectrometer using a 16-bit ADC in the Duke Magnetic Resonance Spectroscopy Center. Samples were loaded into 5-mm NMR tubes with typical volumes of 400–500 μL. All chemical shifts are given in parts per million from DSS referenced against the residual solvent signal. A line broadening of 20 Hz was applied to high spin and 10 Hz to low spin samples to minimize noise. Protein samples were exchanged

into D_2O by being repeatedly (4–5 times) concentrated to about 1 mL on an Amicon filtration device equipped with a PM30 membrane then diluted to 10 mL with 99.9% D_2O (pD = 7.7) SB.

The large sweep widths required the use of short pulses to provide uniform excitation across the entire frequency range. The pulse length needed for uniform excitation is $t_p \leq 1/4SW$. The sweep widths used here were typically about 75 000 Hz requiring pulse lengths of less than 3 μs. The protein samples studied here have 90° pulse times of approximately 12 μs. As a compromise, most experiments used a pulse time of 7.5 μs (57° – 0.83 intensity, uniform over 34 kHz, nulls at 266 kHz). All wide field spectra run had a rolling baseline as a result of unavoidable instrumental dead-time. The baselines were typically flattened by either interpolation, spline fit, or linear tilt subroutines. Nonselective spin lattice relaxation rates were measured using the standard (180°–τ–90°) inversion–recovery method with a composite 180° pulse. Spectra were divided into sections as the 180° pulses used were linear over only a limited spectral range. T_1 relaxation times and errors were calculated utilizing the T1IR GE curve-fitting subroutine. NOE spectra were recorded at 25 °C using a low power pulse from the transmitter to saturate the residual water signal for 45 ms while the decoupler was on resonance; corresponding reference spectra were collected with the decoupler off resonance. On and off resonance spectra were alternated every 512 scans to give a total of 32 000 scans for each. The relaxation delay time used was the water presaturation delay time plus an additional 2-ms delay needed to switch the transmitter from low to high power.

All solid and liquid chemicals were of reagent or analytical grade and unless noted otherwise were not purified further. The DL-cystine-(3,3,3′,3′-d_4) and the EDTA-d_{12} were both obtained from Cambridge Isotope Laboratories.

The protocol used to prepare anaerobic SiR-HP was as outlined previously (Young et al., 1988) with reduction being achieved photochemically using 10 mM EDTA-d_{12} plus either deazaflavin or deazalumiflavin at $^1/_5$ the protein concentration (Massey & Hemmerich, 1978; Janick & Siegel, 1982). After being rendered anaerobic, the protein samples were transferred utilizing a gas-tight syringe to an NMR tube which had been previously flushed with argon and was fitted with a rubber septum. The NMR tube containing anaerobic enzyme–Dlfl–EDTA-d_{12} solution was placed in a chromatography tank filled with ice water (to prevent overheating) and subjected to periods of illumination with a General Electric 200-W Narrow spot sealed beam lamp. At intervals the sample was removed from the bath and optical and/or NMR spectra were recorded. Complete reduction required illumination periods of 30–200 min depending on the sample.

RESULTS

High Spin Ferric Siroheme.[2] The 300-MHz downfield spectrum of high spin ($S = 5/2$) ferric siroheme at pD 6.0 in 50 mM phosphate buffer[3] is given in Figure 3. A total of 36 protons should be present in the siroheme moiety studied, of which 14 peaks with a nominal integrated intensity of 25 protons were detected in the paramagnetic NMR spectrum. The spectrum in Figure 3 was taken to be that of the siroheme monomer as there is evidence of neither line broadening or of anomalous chemical shifts over the temperature (5–35 °C) or concentration (750 μm to 1.5 mM) ranges studied which might correspond to aggregation. All paramagnetically shifted resonances show Curie temperature dependence (Figure 4A). Table II summarizes peak intensity, T_1 measurement, and line width data for the pD 6.0 species. The observed peak widths and temperature dependences are consistent with those of a high spin ferric heme.

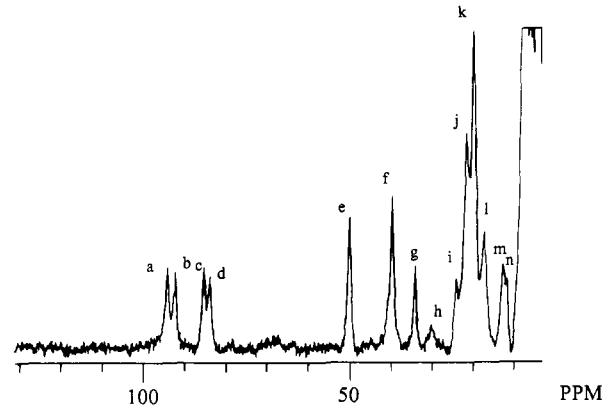

FIGURE 3: ^{1}H NMR spectra at 300 MHz of siroheme in 50 mM KP_i, 99.9% D_2O, at pD 6.0. The spectrum was obtained using the presat pulse sequence with a 200-ms saturation time of the residual water signal and a 7.5-μs observe pulse over 80 000 hertz. A total of 8192 scans was acquired. Only the spectral region from 131 ppm to 0 ppm is displayed.

Two possible coordination numbers exist for high spin ferric hemes; either five-coordinate with one exogenous ligand or six-coordinate with two bound ligands. These two forms can sometimes be distinguished by paramagnetic NMR. Meso proton resonances[4] typically exhibit upfield shifts in five-coordinate iron–porphyrin complexes and downfield shifts in

[2] The initial product of acetone/HCl (0.015 N) heme extraction of SiR (Siegel & Murphy, 1978) appeared to be heterogeneous by optical and HPLC criteria. Therefore, the siroheme used in this study was further purified by HPLC. The purified product gave a single peak by HPLC, and its optical spectrum at pH 6.0 was identical to that reported for siroheme isolated anaerobically from *Desulfovibrio vulgaris* (Kang et al., 1987). However, when the siroheme prepared in this fashion was redissolved in acetone/HCl (0.015 N), the 594-nm α band characteristic of the initially extracted siroheme was not seen, but instead the optical spectrum exhibited a maximum at either 579 or 585 nm depending on whether or not water was present. Possible causes of this discrepancy include aggregation, lactone formation, change in ligand and/or oxidation state, or heme modification during the purification procedure.

[3] The NMR spectrum of siroheme was initially determined in 50 mM phosphate buffer at pD 3.0. The low pH was chosen so as to minimize the possibility of μ-oxo dimer formation (White, 1978). EPR quantitation of the resulting high spin species ($g_\perp = 6.0$, $g_\parallel = 2.0$) was highest at pH 3.0 (0.4 spin/heme vs. 0.2 spin/heme at pH 6.0). There was a systematic shift in the optical spectrum of siroheme as the pH was adjusted from pH 3.0 to pH 6.0. The optical spectra recorded at both these pHs are identical to those reported in the literature (Kang et al., 1987). Addition of potential heme ligands such as chloride or acetate prevented the observed drop in EPR high spin form at higher pH while potassium nitrate did not. However, no change could be detected in the optical spectrum upon anion addition at either pH 3.0 or pH 6.0. The NMR spectrum obtained at pH 3.0 appears to reflect aggregated siroheme as demonstrated by the presence of broad poorly resolved peaks. Since the pK_a of acetyl/propionyl side chains is normally about 4.2, the pD was raised to 6.0 with a small aliquot of NaOD. The resulting increase in the net negative charge of the macrocycle would be expected to prevent aggregation. The observed changes in optical spectra were not consistent, however, with simple π–π aggregation (Shelnutt et al., 1984). The pD 3.0 and pD 6.0 optical and NMR spectra were reversibly interconvertible by the addition of small amounts of either KOD or D_3PO_4. Despite the lower spin concentration at pH 6.0 observed by EPR spectroscopy of frozen samples, the resulting NMR spectral intensity in solution was as strong as that obtained at pH 3.0. This suggests that the lowering of spin intensity with increasing pH along with the observed effect of heme ligands on EPR intensity is probably a result of freezing. While the presence of μ-oxo dimer cannot be excluded (particularly given the low EPR spin intensity), such species typically possess antiferromagnetic coupling and hence exhibit no downfield shifted peaks (Wicholas et al., 1971).

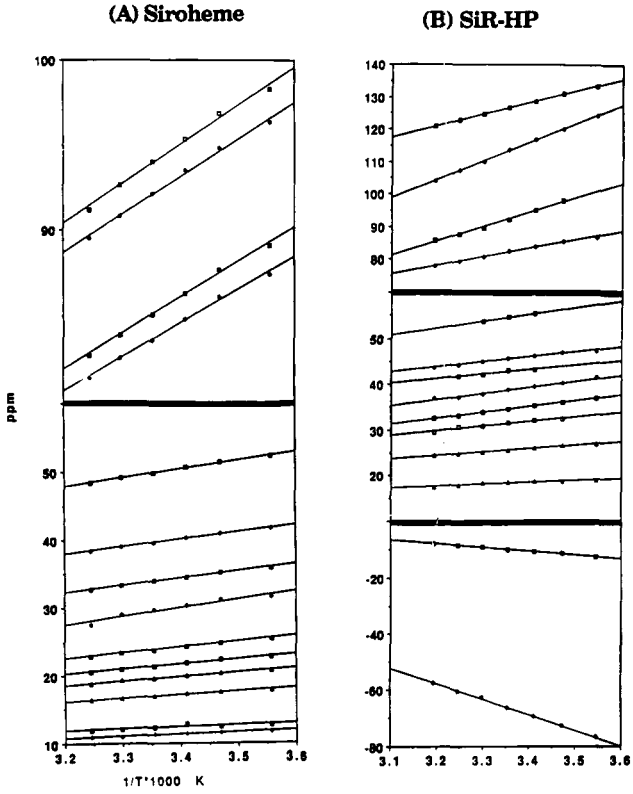

FIGURE 4: Temperature dependence of the paramagnetically shifted resonances in the NMR spectrum of (A) pD 6.0 siroheme in 50 mM KP_i and (B) the hemeprotein subunit of sulfite reductase in 50 mM KP_i at pD 7.7. Spectra were obtained at 300 MHz over the temperature range of 10–35 °C at 5-deg intervals and calibrated vs internal DSS.

six-coordinate complexes (La Mar & Walker, 1979). Siroheme has no observable upfield shifted resonances in the temperature range from 5 to 35 °C,[5] suggesting that, if they are detectable, the meso proton resonances are shifted downfield indicating a six-coordinate siroheme. Meso protons, however, are also readily recognized by their short T_1s. Sullivan et al. (1991) observed for Fe(III)–OEiBC T_1s of 0.4 ms for the upfield shifted five-coordinate meso protons and 0.7 ms for the downfield shifted six-coordinate meso protons. The shortest T_1 observed among the paramagnetically shifted resonances in siroheme is that of the downfield shifted peak *h*, which has a value of 1.2 ms. This T_1 value is more consistent with a pyrroline proton than with a meso proton. Hence, we conclude that no downfield shifted resonance can be assigned to a meso proton. Failure to observe either upfield or downfield shifted resonances arising from meso protons may be due to a combination of large line widths, short T_1s, multiple conformers, and low intensity.[6]

Oxidized SiR-HP Spectra. As isolated, each mole of SiR-HP contains 1 mol of ferric high spin ($S = 5/2$) siroheme and a mole of oxidized [4Fe-4S] cluster in the +2 oxidation state (Siegel et al., 1973; Janick & Siegel, 1982; Han et al., 1989).

Table II: ^{1}H NMR Data for the Paramagnetically Shifted Resonances in $S = 5/2$ Fe(III) Siroheme, pH 6.0

peak[a]	ppm[b]	intensity	T_1 (ms)	peak width[c] (Hz)	$1/T = 0$[d]
a	94.0	1	2.5	285	17
b	92.1	1	2.0	280	18
c	85.1	1	2.7	245	16
d	83.7	1	2.0	300	19
e	49.8	2	2.5	290	7
f	39.5	2	2.7	240	4
g	33.9	1	2.3	215	−0.5
h	29.6	1	1.2	360	−13
i	23.7	14[e]	7.3		−3
j	21.3		5.0		−2
k	19.5				−1
l	16.8				0.3
m	12.2	1			3
n	11.3	1			2

[a] All labels are for the peaks given in Figure 3. [b] Peak position for the sample at 25 °C. Sample referenced against the residual HDO signal at 4.75 ppm. [c] Peak width at half-height in hertz calculated using best Lorentzian fit. [d] Extrapolated intercept at T equals infinity from the temperature dependence data (Figure 4A). [e] Total for peaks i, j, k, and l as they were not fully resolved due to spectral overlap.

The hyperfine shifted resonances in the 300-MHz ^{1}H NMR spectrum of SiR-HP are shown in Figure 5A. A total of 21 hyperfine shifted resonances are detected (Table III) ranging from 130 to −70 ppm with a nominal intensity of 26 protons. Two exchangeable resonances are seen in spectra acquired in H_2O instead of D_2O (Table III). Some skewing of apparent intensities is present in Figure 5A due to the baseline correcting routine. The intensities given in Table III are based on areas taken directly from the uncorrected data. Higher field spectra, run at 500 MHz, showed severe line broadening for all peaks, a result consistent with the presence of the Curie spin effect. All resonances show Curie law temperature dependence (Figure 4B). We postulate (vide infra) that the absence of the characteristic anti-Curie behavior that is normally shown by cysteine protons in $[4Fe\text{-}4S]^{2+}$ clusters may be ascribed to the effect of magnetic coupling between siroheme and cluster.

In order to distinguish iron–sulfur cysteine protons from those arising from the heme periphery, *E. coli* cells were grown on media containing DL-cysteine-(3,3,3′,3′-d_4); SiR-HP isolated from such cells contains deuterium attached to the β-carbon atom of all cysteine residues in the protein. The NMR spectrum of SiR-HP incorporating β-CD_2-cysteine is shown in Figure 5B. Comparison of parts A and B of Figure 5 shows that four peaks (b, c, f, and u) with a total intensity of five protons are missing in the β-CD_2-cysteine-labeled protein.[7] Therefore, these four peaks are assigned to the β-CH_2s of cluster cysteines. The absence of any NOEs between these peaks suggests that they belong to separate cysteines and are not geminal partners. Peak b shows a NOE

[4] The following standard nomenclature is used in describing siroheme protons. Meso protons are directly bound to the ring at positions 5, 10, 15, and 20 (Figure 1). The two adjacent partially saturated rings characteristic of an isobacteriochlorin are the pyrroline rings. The protons directly bound at positions 3 and 8 of siroheme are the pyrroline protons. The two other classes of protons bound to the pyrroline rings are in the pyrroline methyls and the pyrroline methylenes. The two unsaturated pyrrole rings possess only substituent protons due to methylene groups in siroheme.

[5] Higher temperatures often yield peaks with smaller line widths. This makes it easier to detect the otherwise broad meso resonances.

[6] To further study the coordination number of siroheme, chloride was added to siroheme in phosphate buffer as chloride heme complexes are typically five-coordinate. The addition of a concentrated solution of KCl (final chloride concentration 100 mM) to the siroheme solution in phosphate buffer caused no change in siroheme's NMR or optical spectra. The absence of perturbation upon the addition of chloride suggests that siroheme in phosphate buffer at pH 6.0 is already five-coordinate. However, since there is no evidence for chloride ligation of siroheme in solution, the lack of spectral perturbation may instead be due to the absence of binding.

[7] Careful examination of the spectra in Figure 5A,B indicates small differences in peaks d/e and h/i. Review of the uncorrected data shows that the differences in h/i are artifacts resulting from the baseline correction routine. The small changes in d/e cannot be well resolved due to the low signal-to-noise present in the deuterated cystine sample along with a rolling baseline.

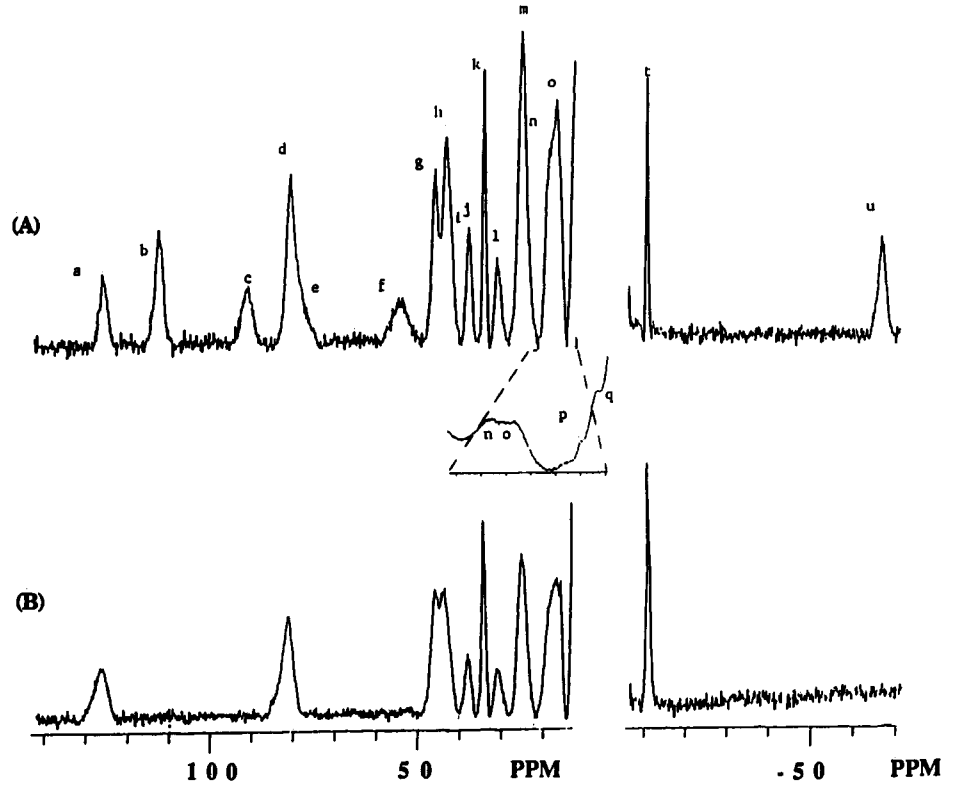

FIGURE 5: (A) 1.3 mM sulfite reductase hemeprotein in 99.9% D_2O, pD 7.7, SB. The spectrum was obtained with a sweep width of 75 000 Hz, 60-ms water saturation time, 7.5-μs observe pulse collected into a 16K double precision file on a GN 300 MHz instrument. A total of 32 000 scans was acquired. The inset shows an expansion of the 22–10 ppm region. (B) Spectrum of 1.6 mM sulfite reductase from cells grown on deuterated cystine prepared in parallel and run under identical conditions.

Table III: ^{1}H NMR Data for the Paramagnetically Shifted Resonances in Oxidized SiR-HP

peak[a]	ppm[b]	relative intensity	T_1 (ms)	peak width[c] (Hz)	$1/T = 0$[d] (ppm)	NOE to peak	assignment
a	126.5	1	2.9	590	6	i, o, q	17a, 13a
b	113.5[e]	1	3.6	525	−79	k	β-cysteine
c	92.1[e]	1	1.2	685	−55		β-cysteine
d	82.4		3.3		−4	g, l	
e	78.2						
f	54.6[e]	1	1.3	900	4	g, j, m	β-cysteine
g	45.8	1	5.8		8	j, m	2a, 3a, 7a, 8a
h	43.1	1	5.6		9		2a, 3a, 7a, 8a
i	41.9	1				a	17a, 13a
j	38.8	1	7.3	355	−8	f	
k	34.7	1	5.0	225	−10	b	α-cysteine
l	31.7	1	2.5	430	−4	e	2a, 3a, 7a, 8a
m	25.6	4	4.2	545	−1	e, f	methyls+
n	19.2	1			4		
o	17.2	1				a, i, q	17b, 13b
p	12.1	1					
q	10.8	1				a, i, o	17b, 13b
r	10.7[f]	1					
s	10.1[f]	1					
t	−9.9	1	4.2	162	32	u	α-cysteine
u	−66.3[e]	2	2.8	673	120	t	β-cysteine

[a] All labels are for the peaks given in Figure 5A. [b] Peak position for the sample at 25 °C in 50 mM KP_i, pD 7.7. Sample referenced against internal DSS. [c] Peak width at half height in hertz calculated using best Lorentzian fit. [d] Extrapolated intercept at T equals infinity from the temperature dependence data (Figure 4). [e] Assigned to β-CH_2 protons of cysteine by deuterium labeling. [f] Exchangeable protons seen in H_2O but not D_2O.

to peak k and peak u to peak t (Figure 6). Besides exhibiting no other NOEs, both peaks k and t have relatively narrow line widths as well as smaller hyperfine shifts when compared to the β-CH_2 protons. For these reasons, resonances k and t are tentatively assigned as cysteine α-CH protons. The magnitude of the hyperfine shifts arising from protons of the cysteine residues in SiR-HP is much greater than has previously been described for analogous protons in isolated $[4Fe\text{-}4S]^{2+}$ clusters (Table IV; Poe et al., 1970; Packer et al., 1977) and is also much greater than would be expected due to dipolar coupling between heme and cluster (Satterlee, 1986). In our view, the data require the existence of a bridge between the high spin ferric siroheme and the $[4Fe\text{-}4S]^{2+}$ in SiR-HP solution and it is this bridge that gives rise to the observed spin coupling between the prosthetic groups. This interpretation is in good agreement with results obtained with frozen solutions of SiR-HP by Mossbauer (Christner et al., 1981), ENDOR (Cline et al., 1985), and by resonance Raman (Han et al., 1989a) spectroscopic studies.

Almost all of the remaining resonances can be plausibly assigned to either siroheme side chain protons or the two as yet unassigned cysteine α-CHs. Peak a shows NOEs (Figure

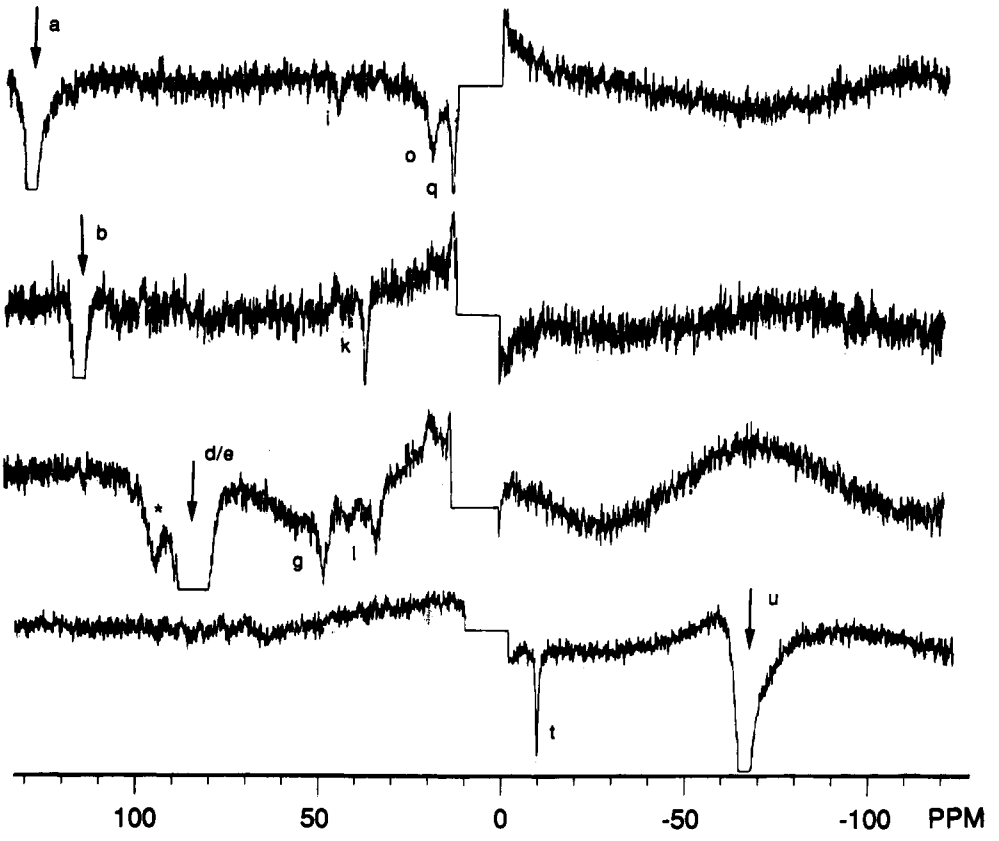

FIGURE 6: One-dimensional NOE experiments on oxidized SiR-HP. NOE difference spectra were generated by subtracting the reference spectrum at 300 MHz with the decoupler off resonance from a similar spectrum of the sample in which the desired resonance was saturated. In each of the traces presented, a downward arrow indicates a peak being saturated. In the third trace, both peaks d and e are saturated along with some slight spillover to peak c (*). The noisy diamagnetic 0–10 ppm region has been blanked. The peaks are labeled as in Figure 5A.

Table IV: Summary of ^{1}H Peak Positions for Cysteine β-CH_2s of SiR and Other Iron–Sulfur-Containing Proteins

compound	ppm	reference[a]
	Sulfite Reductase Hemeprotein Subunit	
SiR-HP	113.5, 92.1, 54.6, −66.3, −66.3	1
SiR-HP^{1-}	130.8, 94.8, 22.7, −71.2, −71.4	1
SiR-HP^{2-}	111.7, 75.8, 55.7, 45.2, 45.2, −27.6, −57.2	1
	Oxidized Ferredoxins $[4Fe\text{-}4S]^{2+}$	
C. pasteurianum	17.3, 16.2, 16.0, 14.9, 13.6, 12.5, 12.2, 11.2, 9.6, 9.6, 9.1, 8.15, 7.7, 65.	2
C. acid-urici	16.2, 15.3, 15.1, 13.3, 12.1, 11.1, 10.8	3
	Reduced Ferredoxins	
Bacillus polymixa	36.8, 35, 32.9, 22.2, 19.8, 17, 15.9, 13.8	4
C. pasteurianum	60.2, 57.0, 54.6, 40.7, 38.8, 33.7, 28.2, 26.9, 25.8, 22.0, 20.3, 17.2, 15.8, 14.4, 12.0	5
	Reduced HiPiPs $[4Fe\text{-}4S]^{2+}$	
C. vinosum	16.8, 15.9, 12.7, 11.6, 10.7, 7.7, 7.2, 5.3	6
C. gracile	16.2, 16.2, 12.6, 10.8, 10.0	7
	Oxidized HiPiPs $[4Fe\text{-}4S]^{3+}$	
C. vinosum	110.6, 40.10, 37.5, 30.4, 24.2, 23.7, −35.6, −35.9	7
R. gelatinosa	95.8, 45.1, 39.6, 31.9, 13.0, 11.9, −24.8, −30.9	8
E. halophilia I	92.1, 46.8, 42.3, 29.0, 15.6, −20.8, −26.3	9
E. halophilia II	93.8, 57.8, 48.2, 48.0, −13.2, −16.8, −20.1, −23.5	9, 10
E. vacuolata I	101.4, 32.5, 30.1, 26.1, 25.1, 23.2, −12.1, −25.5	9
E. vacuolata II	104.8, 32.5, 29.8, 25.2, 23.9, 22.8, −15.9, −25.5	9
	Reduced $[2Fe\text{-}2S]$	
P. umbilicalis	130.9, 122.6, 103.8, 97.5, 27.6, 26.7, 22.0, 18.6	11
S. platenis	134.4, 124.9, 103.2, 97.4, 26.4, 25.8, 21.1, 17.9	11

[a] References: (1) this work. (2) Poe et al., 1970.* (3) Packer et al., 1977. (4) Phillips et al., 1974.* (5) Bertini et al., 1992.* (6)Bertini et al., 1991. (7) Sola et al., 1989.* (8) Banci et al., 1991. (9) Krishnamoorthi et al., 1986.* (10) Banci et al., 1991. (11) Dugad et al., 1990; Skjeldal et al., 1991. An asterisk indicates β-CH_2 and α-CH protons not resolved.

6) to three peaks: i, o, and q. The α-CH_2 partners of a propionate bound directly to the ring are expected to have much larger shifts than the β-CH_2 protons. For this reason, peaks a and i are interpreted as belonging to a propionate α-CH_2 while peaks o and q are the β-CH_2 partners. Sullivan et al. (1991) observed larger shifts in five-coordinate Fe(III)–OEiBC for pyrrole than pyrroline protons. If this model holds for siroheme, the propionate is at either position 17 or 13 of siroheme (Figure 1). The NOEs from the overlapping peaks d and e could not be resolved because saturation of either one

alone was not possible. Peaks d and e show NOEs to peaks g and l. Of all the paramagnetically shifted resonances, only peak m has sufficient intensity to represent a freely rotating methyl group. Peak f, besides being identified as arising from a cysteine β-CH_2, has NOEs to three other protons (g, j, m) (Kaufman et al., 1993). Both of these protons show multiple NOEs to other paramagnetically shifted resonances (Table III), a result which identifies them as belonging to the siroheme ring side chains.

Reduction of SiR-HP. In order to observe the intermediate one-electron and fully reduced (two-electron) states, we subjected an anaerobic sample of SiR-HP (containing 10 mM EDTA-d_{12} and 150 μM of deazalumiflavin), in a sealed NMR tube, to photoreduction for short successive periods of time. The progress of the photoreduction was monitored optically by placing the tube in a holder which allows direct optical spectroscopy on a sample within an NMR tube. Due to the high concentration of enzyme, we could only observe the loss of the charge transfer peak at 712 nm. From the area of this peak, the percentage of high spin siroheme present could be directly measured, and the amount of 1-electron and 2-electron reduced enzyme present was calculated from the published heme and cluster midpoint potentials (–340 mV and –405 mV; Janick & Siegel, 1982). Figure 7 shows a section of the resulting NMR titration along with the amount of each species as determined optically. Illumination was continued until no further change was detected in the NMR spectrum. Figure 8 gives the downfield and upfield shifted regions of all three redox states. Due to the small separation of siroheme and cluster midpoint potentials, no pure SiR-HP^{1-} could be isolated. The spectrum shown in Figure 8B is highly enriched in the intermediate form, with peaks due to the 1-electron state labeled by asterisks. After complete reduction, the sample was reoxidized by opening to air; and an NMR spectrum identical to the starting spectrum was obtained. To determine whether resonances arise from the heme or the cluster, a β-CD_2-deuterated cysteine sample was also photoreduced; the resulting spectra are shown in Figure 9. As can be seen by comparing Figures 8B and 9, the 1-electron reduced SiR-HP has three proton peaks shifted downfield and two shifted upfield that are seen to disappear on deuterium incorporation. The remaining peaks must therefore be due to protons associated with the heme. As discussed below, their pattern of shifts is consistent with a $S = 1$ ferrous heme (Goff & La Mar, 1977; Medhi et al., 1989; Stolzenberg et al., 1981). On full reduction six peaks are found in unlabeled SiR-HP (with a nominal intensity of seven protons) which are missing in enzyme containing β-CD_2-cysteine. The siroheme moiety is now in the $S = 2$ high spin ferrous state (Han et al., 1989a).[8]

pD Titration of Oxidized SiR-HP. The effect of pD on the NMR spectra of oxidized SiR-HP was measured in the range pD 6.0–9.9 at both low and high ionic strength. The pD of a sample in 100 mM KP_i (pD 7.7) was adjusted using small amounts of either dilute KOD or D_3PO_4. While the spectral changes on changing the pD are completely reversible at low pD (<6.5), the sample was less stable than at higher pD, with the enzyme exhibiting a tendency to precipitate out of solution; therefore, the sample was centrifuged after every pD change. Peak position was referenced against internal DSS and the data curve was fit (Figure 10) using the SYSSTAT data analysis package [Sysstat Inc., Evanston, IL (1989)] on a Macintosh computer. The proton resonances showed a variable degree of pD dependency. While resonances a, c, e, and i showed almost no change, peak h experienced a 10 ppm shift while the other peaks showed small changes (~1 ppm net shifts). The data could be fit to a single pK in the range of 6.5–6.9 (Figure 10).[9]

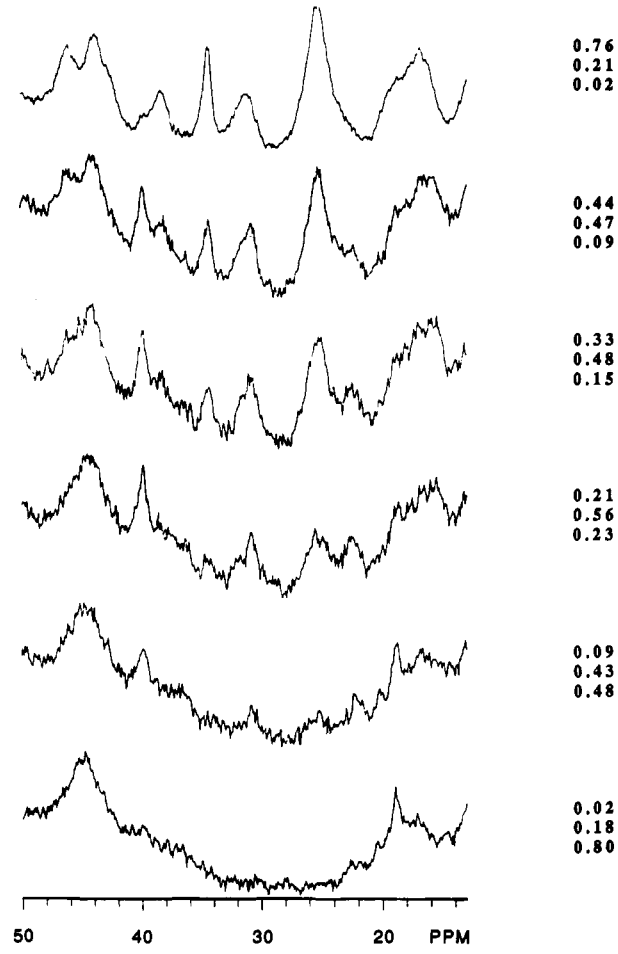

FIGURE 7: Reduction of 1.6 mM sulfite reductase hemeprotein in 99.9% D_2O, pD 7.7, with 10 mM EDTA-d_{12} and 150 μM Dlfl monitored both optically and by NMR. The 50–13.5 ppm sections of the paramagnetic NMR spectra at 300 MHz are shown from top to bottom following 10, 30, 40, 50, 60, and 90 min of illumination within a sealed NMR tube. At each time point an optical spectrum was also run and the amount of high spin siroheme present was determined by the absorbance at 712 nm. Using the Nernst equation with $n = 1$ and midpoint potentials of –340 mV and –405 mV for heme and cluster, respectively (Janick et al., 1983), the amount of 1-electron and fully reduced enzyme present was calculated. The three numbers corresponding to proportions of SiR-HP, SiR-HP^{1-}, and SiR-HP^{2-} are presented next to each spectra. The accuracy is no greater than ±10% for the amount of high spin present due to the variability of absorption readings within a curved NMR tube. This can lead to very large errors in the amount of SiR-HP^{1-} and SiR-HP^{2-} present at low concentrations of oxidized enzyme.

DISCUSSION

Analysis of Cluster Shifts in SiR-HP. Previous studies of the iron–sulfur cluster in SiR-HP have unambiguously identified the cluster as belonging to the low potential [4Fe-4S] type on the basis of nonheme iron/acid labile sulfide

[8] Model complexes of thiolates ligated to high spin ferrous hemes (Lukat et al., 1990) have the β-CH_2 groups of the thiolate ligand extending as far as 260 ppm downfield. We have examined spectra of SiR-HP^{2-} as far as 300 ppm downfield without detecting any additional resonances.

[9] To rule out ionic strength effects, the experiment was repeated in the presence of 0.5 M potassium nitrate. The high ionic strength caused the apparent pK_as to decrease by 0.2–0.3 of a pD unit. Accurate calculation of the pK_a at high ionic strength was not possible because the lower portion of the sigmoidal curve could not be reached due to enzyme instability at lower pD.

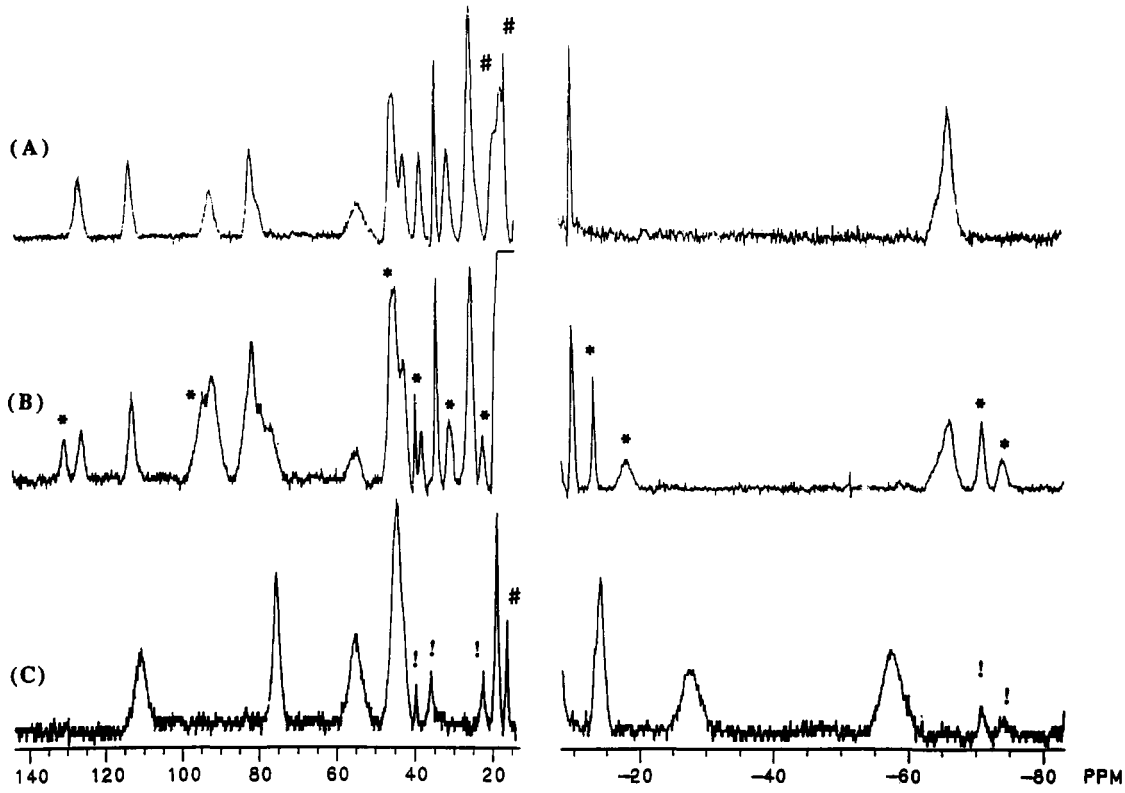

FIGURE 8: Downfield and upfield regions of the NMR spectra at 300 MHz of 1.4 mM unligated sulfite reductase hemeprotein subunit in 90% H_2O in all three possible redox states. Spectrum A corresponds to the fully oxidized enzyme with the two exchangeable peaks marked. Due to the closeness of midpoint potentials, no pure 1-electron state could be achieved. Spectrum B consists predominantly of the fully oxidized and 1-electron reduced states with the latter peaks indicated by asterisks. Spectrum C is the fully reduced enzyme with a small amount of impurity from higher oxidation states labeled by (!). Exchangeable peaks are indicated by a (#) sign.

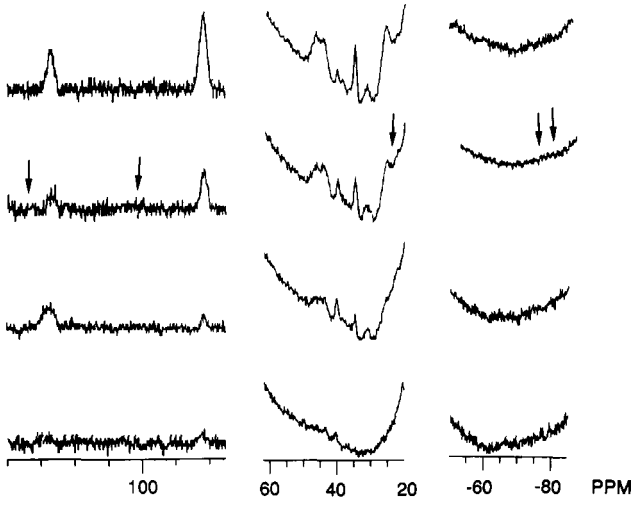

FIGURE 9: Reduction of deuteriocysteine-labeled SiRHP monitored by NMR spectroscopy at 300 MHz from more oxidized (top) to less. Three sections of the spectrum from 140 to 75, 60 to 20, and −50 to −85 ppm are displayed with the location of peaks present in the spectrum of unlabeled SiR-HP^{1-} indicated by arrows.

stoichiometry (Siegel et al., 1973, 1982) and EPR (Janick et al., 1982), resonance Raman (Han et al., 1989a), and Mossbauer spectroscopy (Christner et al., 1981, 1983a,b). The cluster exists at the $[4Fe\text{-}4S]^{2+}$ oxidation level in resting and 1-electron reduced SiR-HP and at the $[4Fe\text{-}4S]^{1+}$ oxidation state in 2-electron reduced enzyme (Christner et al., 1981, 1983b; Madden et al., 1989). Paramagnetic NMR spectroscopy is often useful for investigating the structure and electronic properties of iron–sulfur proteins since the patterns of hyperfine shifted resonances and their temperature dependences can provide detailed information on bonding and magnetic interactions within a cluster. The spectra of a number of [4Fe-4S] proteins have been previously reported (Packer et al., 1977; Sola et al., 1987). For all such clusters examined so far, NMR resonances arising from those amino acids nearest the cluster are shifted outside the diamagnetic region as a result of paramagnetism. This hyperfine shift is most prominent for the strongly paramagnetic $[4Fe\text{-}4S]^{1+}$ and $[4Fe\text{-}4S]^{3+}$ clusters, but substantial downfield shift also arises from the residual paramagnetism of the $[4Fe\text{-}4S]^{2+}$ center due to the population of low lying excited states at room temperature. The downfield shifted amino acid resonances associated with $[4Fe\text{-}4S]^{2+}$ centers have all been observed in the range of 8–20 ppm (Packer et al., 1977; Skjeldal et al., 1989; Poe et al., 1970). Only residues coordinated to clusters in the +3 oxidation state have been shown to have both upfield and downfield shifts (Banci et al., 1991). The hyperfine shift in clusters is believed to arise predominantly from contact interactions (Poe et al., 1970) derived via either a σ or π bond delocalization mechanism. Sulfur is considered to exhibit sp^2 hybridization and, as a result of coordination to iron, spin density is transferred to the nonbonding π-orbital perpendicular to the plane of the sp^2 orbitals. When cysteine is the coordinating ligand, the β-CH_2 protons can sense this spin density by hyperconjugation and manifest a π contact shift (Poe et al., 1970). If free rotation about the C–S bond existed, the two β-CH_2 protons would be shifted equally, since on average their positions relative to the spin density centered on the sulfur would be equivalent. While this is the case for synthetic model compounds (Holmes et al., 1979), in proteins the two β-CH_2 protons are generally fixed in space and positioned nonequivalently, resulting in discrete resonances.

Ignoring for a moment the effect of coupling between cluster and siroheme, we would expect to detect in oxidized SiR-HP

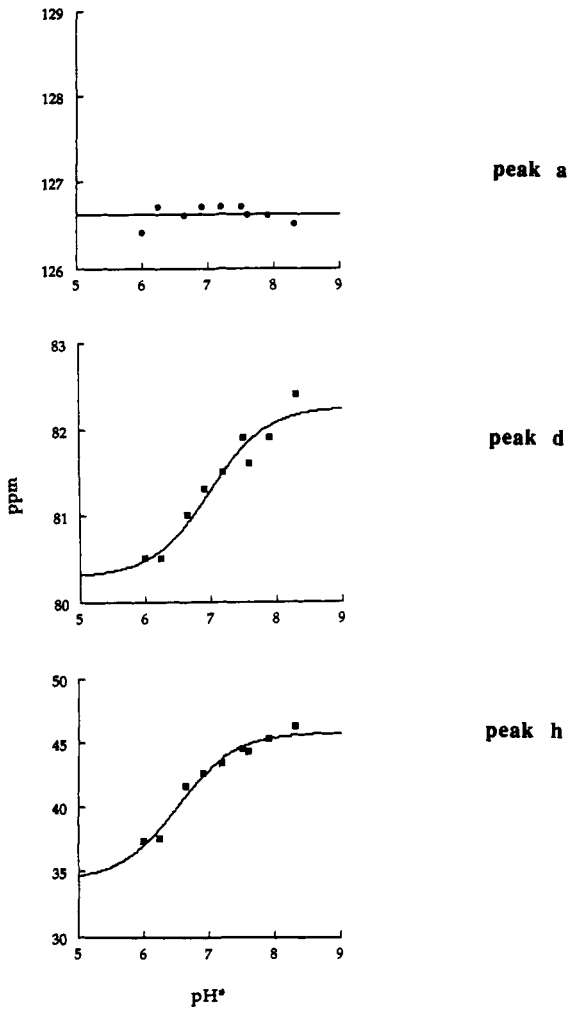

FIGURE 10: Analysis of the pH titration data. The first graph is for peak a whose chemical shift is essentially pH independent. The second graph is for peak d which shows a typical small pH dependence. The third graph is for peak h which has the largest pH dependence. The curves for d and h are the best calculated fit using the Sys Stat data package on a Macintosh computer. The calculated pK_as are 6.5 ± 0.5 and 6.9 ± 0.4, respectively.

four to eight β-CH_2 resonances from the cysteines coordinated to the cluster, all within the 8–20 ppm range. Instead, three β-CH_2 cysteine resonances of unit intensity are observed much farther downfield, and a single resonance with twice the intensity is observed upfield. Such large shifts demonstrate that the shifted resonances are being influenced by the paramagnetic siroheme Fe(III) and that through bond coupling must exist between the siroheme and cluster in solution. If the cluster were simply in close proximity to the heme ring, dipolar shifts of this magnitude would not be observed, since high spin ferric iron has a totally symmetric electronic ground state yielding very small dipolar shifts (Satterlee, 1986). The large hyperfine shifts seen must be contact in nature, requiring that spin density be transferred from the siroheme iron to the cluster via an exchange pathway. Although resonance Raman data of Madden et al. (1989) have suggested that a sulfur atom is linked to both heme and cluster iron atoms in SiR-HP in solution, the present data provide the first evidence that this is due to a cysteine residue of the protein.

The four resonances assigned to cysteine β-CH_2s all show Curie temperature dependence but possess $1/T$ intercepts far outside the diamagnetic region (Table III). The absence of anti-Curie type behavior that is typically observed from the cysteine protons of oxidized ferredoxins can be ascribed to exchange-coupling between siroheme and cluster. In isolated [4Fe-4S] clusters, hyperfine shifts are present despite the fact that the cluster is nominally diamagnetic due to the population of excited states at room temperature. As the sample temperature is lowered, the excited state population drops and the net paramagnetic shift decreases. This is the reverse of the normal Curie law behavior in which larger hyperfine shifts are seen at lower temperature. The Curie temperature behavior seen for cysteine residues in SiR can be accounted for by the large amount of spin density transferred from the high spin ferric siroheme iron to the cluster. Further evidence for coupling between prosthetic groups is that cluster resonances, like siroheme derived protons, also show severe Curie spin effect broadening at higher magnetic fields. Since isolated clusters are typically low spin and the Curie spin effect depends on the square of the effective spin, the presence of Curie line broadening for cysteine protons shows that the cluster directly senses the siroheme high spin iron.

Oxidized SiR-HP not only possesses downfield shifted cysteine resonances but also has an upfield shifted resonance derived from the β-CH_2 protons of a cluster cysteine. The observation of upfield shifted resonances from [4Fe-4S] clusters has only previously been reported for HiPiPs in the +3 (paramagnetic) oxidation state. These systems have been observed to have either two or four upfield shifted resonances (Bertini et al., 1991). No isolated [4Fe-4S] clusters in the +2 oxidation state have been observed to possess upfield shifted cysteine resonances. The presence of such an upfield shifted resonance in oxidized SiR is further evidence that coupling between heme and cluster exists in solution. The presence of upfield shifts is consistent with the coupling model described below.

The large size of hyperfine shifts, absence of anti-Curie temperature dependence, presence of Curie spin effect, and observation of upfield shifts for cluster cysteine resonances are presented here as evidence for coupling in solution. An alternative hypothesis may be that the [4Fe-4S] cluster in SiR has an unusual structure which causes these observed perturbations from the typical [4Fe-4S] cluster NMR spectrum. Several lines of evidence, however, argue very strongly against this hypothesis. Resonance Raman (Han et al., 1989a) and Mossbauer (Christner et al., 1981) studies and X-ray crystallography (McRee et al., 1986) on resting SiR-HP all yield the results expected of a [4Fe-4S] cluster in the +2 oxidation state. While it is not possible to study the cluster of SiR-HP in isolation, the binding of cyanide along with the addition of one equivalent of electrons yields a ferrous S = 0 siroheme which does not perturb the cluster (Christner et al., 1983b). The NMR spectrum of this species matches that of a typical uncoupled $[4Fe\text{-}4S]^{2+}$ cluster (J. Kaufman, L. M. Siegel, and L. D. Spicer, manuscript in preparation).

All four resonances arising from the cluster β-CH_2s have been assigned to separate cysteines, since no NOEs were detected among them which might represent coupling between geminal protons. It should be pointed out, however, that the shorter the T_1 and T_2 of a peak, the more difficult it is to detect NOEs from that peak (Lecomte et al., 1991). Peaks c and f have large line widths with short T_1s, which might account for their lack of NOEs although peak f shows multiple NOE couplings to the heme ring (Kaufman et al., 1993). The upfield shifted resonance has double intensity, suggesting it either arises from the overlap of two proton signals from separate cysteines or represents a geminal pair of β-CH_2 protons with identical shifts. Given the absence of NOEs, the upfield peak is taken to represent a geminal pair because

otherwise the presence of five cysteines showing paramagnetic shifts must be invoked to explain the data. The assignment of peak u to a geminal pair is also consistent with the model discussed below, while the other possibility, assignment to two separate cysteines, is inconsistent with this model. The geminal partners of resonances b, c, and f, which are not observed, either may not be shifted out of the diamagnetic region or more likely are so broad that they remain undetected.

Although it represents a rather poor approximation to physical reality, a model which takes into account the exchange interaction between the two prosthetic groups of SiR-HP has been suggested previously by Christner et al. (1981); this model can in fact explain the unusual properties of cluster proton NMR resonances in SiR-HP. Mossbauer studies on frozen SiR-HP revealed pairwise nearly equivalent iron sites arising from the cluster (Christner et al., 1981). Resonance Raman data suggest that the resting enzyme behaves identically in solution and the frozen state (Han et al., 1989a). Instead of treating the still intractable problem of coupling a [4Fe-4S] center to a heme Fe, Christner et al. (1981) utilized a simpler system in which an oxidized diamagnetic [2Fe-2S] cluster is coupled to siroheme with each iron representing an equivalent pair (Munck, 1982). While we recognize the limitations of using a [2Fe-2S] cluster to approximate a [4Fe-4S] cluster, especially given their fairly different NMR spectra (Poe et al., 1970; Packer et al., 1977; Skjeldal et al., 1991), we believe that the simplified model can (as described below) yield useful insights into the interpretation of the observed NMR spectra.

In this model, the cluster is divided into two iron sites, of which iron site 1 is coupled both to cluster site 2 and to the heme. Magnetic hyperfine terms of the form $A_j S_h I_j$, where $S_h = 5/2$ and where the subscript j denotes the iron sites, can be used to express the exchange interaction. With $\mathbf{S}_c = 0$ (the cluster spin) and the assumption that the heme cluster exchange coupling is small compared to $J\mathbf{S}_1\mathbf{S}_2$ (the cluster internal coupling) but large compared to the Zeeman and hyperfine terms, the desired spin Hamiltonian is given by

$$\mathbf{H} = g_c\beta\mathbf{H}\mathbf{S}_h + A^c{}_h\mathbf{S}_h\mathbf{I}_h + A_1\mathbf{S}_h\mathbf{I}_1 + A_2\mathbf{S}_h\mathbf{I}_2 \qquad (1)$$

where the isotropic terms $A^c{}_h$, A_1, and A_2 represent the amount of coupling between the $S = 5/2$ heme iron and the heme, site 1, and site 2 of the cluster, respectively. These values, as determined by both Mossbauer (Christner et al., 1981, 1983a) and ENDOR (Cline et al., 1985), are, respectively, −27 MHz, +6.2 MHz, and −6.1 MHz. The alteration in sign is due to the alignment of $\mathbf{S}_1$ antiparallel to $\mathbf{S}_h$. The strong internal coupling $J\mathbf{S}_1\mathbf{S}_2$ in turn orients $\mathbf{S}_2$ antiparallel to $\mathbf{S}_1$, and thus parallel to $\mathbf{S}_h$. The observed NMR hyperfine shift of cysteine C_β protons not only reflects on the magnitude and sign of the spin density transferred to the iron $\langle Sz \rangle$ but also has an angular dependence via the following equations:

$$\delta_{con} = \langle Sz \rangle D f(\phi_i) \qquad (2)$$

with

$$f(\phi_i) = b_0 + b_2 \cos^2 \phi_i \qquad (3)$$

Since D, b_0, and b_2 are positive constants and the angular term $\cos^2 \phi_i$ is always positive, the direction of paramagnetic shift will depend solely on the sign of spin density at the coordinated iron. Hence if the two irons in SiR corresponding to site 2 in the model possess negative spin density, their coordinated cysteines will show downfield shifts, while site 1 irons will have positive spin density, yielding upfield shifted resonances. However, the bridging cysteine will experience both positive spin density from site 1 and negative spin density from the heme. Its net hyperfine shift therefore will depend on which spin density predominates at the bridging sulfur atom. Given the expected greater spin density on the heme as opposed to that at site 1, a net downfield shift can be expected which would be modulated by its angular dependence. The dipolar contribution to the observed isotropic shift of the heme ligand is small relative to the contact shift, since high spin ferric ions possess a totally symmetric electronic ground state with an isotropic **g** tensor (Satterlee, 1986). Peak f fits this model in possessing a downfield shift and having a large line width with the short T_1 (expected for a heme ligand). Most importantly, peak f has multiple NOEs to the heme ring. Examination of the preliminary X-ray crystallographic structure of SiR-HP (McRee et al., 1986) shows that, in addition to the bridging ligand, the only other cluster-ligated cysteine that can possibly come close enough to the siroheme ring to exhibit NOEs is that one coordinated to the face of the cluster toward the siroheme ring but that is not the bridging ligand. With the current data it is not possible to clearly distinguish between these two possibilities. However, another observation which also supports cysteine as the bridging ligand between cluster and heme is the absence of geminal NOEs among the four cysteine protons. If another amino acid were acting as the bridge, only three paramagnetically shifted cysteine resonances would be detected. The short T_1, large line width, downfield chemical shift, heme NOEs, and correspondence to the above model all are consistent with the assignment of resonance f to the bridging ligand.

The other two downfield shifted peaks (b and c) can now be interpreted as representing cysteines bound to site 2 while the upfield resonance (peak u) arises from the nonbridging cysteine of site 1. Since the coupling constants for site 1 and site 2 from the Mossbauer data have nearly equal magnitude but opposite sign (Christner et al., 1981), the isotropic shifts[10] of the coordinated cysteines are expected to be equal but opposite in sign. This result is not observed, as the downfield shifted resonances from site 2 have much larger isotropic shifts than the nonbridging cysteine from site 1 (see Table IV). This inequality could be interpreted as arising from differing angular dependencies (see eqs 2 and 3).

If the downfield shifted peaks b, c, and k (α-CH cysteine proton identified from NOE experiments, Figure 6) attributed to cluster site 2 are examined by themselves, they are remarkably similar to the spectra of the reduced [2Fe-2S] ferredoxins from *Porphyra umbilicalis* and *Spirulina platensis*. These reduced [2Fe-2S] clusters consist of a ferric iron, coordinated to two cysteines, which is bridged via two sulfides to an Fe(II) also coordinated to two cysteines. The NMR spectra of these clusters have four downfield shifted β-CH_2 resonances in the 140–90 ppm range (Table IV) from the two cysteines coordinated to the Fe(III), with a single α-CH peak at 43 ppm having a T_1 of only 5.4 ms (Dugad et al., 1990; Skjeldal et al., 1991). Two of these resonances are extremely broad, with short T_1s (0.4 ms), and the other two are much sharper, with longer T_1s (1.5 ms). While no interproton NOEs could be observed, by analogy with the crystal structures of these ferredoxins, it was suggested that the geminal pairs consist of a mixture of the sharp and broad peaks with the broad peak being due to the protons that are much closer to the iron. While the corresponding two broad

[10] The difference between the observed paramagnetic shift and the corresponding resonance in an equivalent diamagnetic compound is the isotropic shift. For cysteine β-CH_2s, the diamagnetic shift is approximately 3.0 ppm, which means peak b at 113.5 ppm has an isotropic shift of 110.5 ppm and peak u at −63.3 ppm has an isotropic shift of −66.3 ppm.

peaks have not been observed in SiR-HP (possibly due to the combination of greater molecular weight and Curie line broadening present in SiR-HP), two nongeminal, sharp β-CH_2 peaks are present, at 113.5 and 92.1, with a single α-CH, at 34.7 ppm, having a longitudinal relaxation time of 5.0 ms. This interpretation is also consistent with Mossbauer studies, in that site 2 was interpreted by Christner et al. (1981) to possess ferric character.

One-Electron Reduced SiR-HP. Spectra arising upon successive stages of photoreduction of oxidized SiR-HP permit us to study the intermediate and fully reduced forms of the enzyme. By a combination of optical, resonance Raman, Mossbauer, and EPR spectroscopies (Christner et al., 1981; Janick & Siegel, 1983; Madden et al., 1989), it has been clearly demonstrated that the first electron is added to the heme, generating an EPR silent form, while the second electron reduces the cluster. Resonance Raman spectra (Han et al., 1989a) of the 1-electron form in solution showed that the heme was in either the low or intermediate spin ferrous form. Mossbauer measurements on SiR-HP^{1-} have indicated that the siroheme Fe(II) is either intermediate or high spin in the frozen state. Taken together, these data suggest that the heme is in the ferrous $S = 1$ intermediate spin state. However, inability to successfully prepare frozen samples of SiR-HP^{1-} for Raman spectroscopy meant a spin state transition from low spin ferrous siroheme to the intermediate or high spin state on freezing could not be excluded.

Several paramagnetic NMR studies have characterized the properties of intermediate and high spin ferrous hemes in solution (Medhi et al., 1989; Goff & La Mar, 1977; Goff et al., 1977). A clear spectral change in such hemes is observed on going from the intermediate to the high spin ferrous forms. The four-coordinate intermediate spin complexes show the meso protons at about 70 ppm, while the ring methyls and methylenes appear in the range of 30–70 ppm. High spin ferrous hemes with 2-methylimidazole as ligand show much smaller isotropic shifts, with all paramagnetically shifted resonances in the range of 10–22 ppm (Medhi et al., 1989). Examination of NMR spectra of the enzyme at various stages of photoreduction of SiR-HP (Figures 7 and 8) clearly shows peaks appearing downfield of 20 ppm. Photoreduction of SiR-HP containing β-CD_2 cysteine identified five single intensity peaks at 130.8, 94.8, 22.7, –71.2, and –71.4 as belonging to protons of cysteines associated with the cluster. After cluster derived peaks were excluded, resonances in the range of 30–50 ppm are still observed for SiR-HP^{1-}; therefore, by comparison to the spectra of ferrous porphyrins, siroheme can be identified as belonging to the intermediate ferrous $S = 1$ state in solution. However, siroheme is an isobacteriochlorin and not a porphyrin; it is quite possible that reduced hydroporphyrins yield different spectra than do porphyrins. Unfortunately, no ferrous isobacteriochlorin NMR studies have as yet been reported. Several studies on isolated synthetic intermediate spin ferrous chlorins (Stolzenberg et al., 1981; Strauss & Pawlick, 1986) have appeared in the literature, and recently the spectra of high spin ferrous chlorins incorporated into myoglobin have also been reported (Keating et al., 1992). The pattern and magnitude of isotropic shifts for the $S = 1$ ferrous chlorins reported so far appear similar to those for porphyrins (Stolzenberg et al., 1981; Strauss & Pawlick, 1986) in spite of the fact that chlorins possess significantly different electronic structures than do porphyrins (Strauss et al., 1985). For the high spin ferrous chlorins, numerous differences from the pattern of hyperfine shifts reported with porphyrins were observed (Keating et al., 1992). The meso protons showed large downfield shifts into the 50–30 ppm range with protons attached to the reduced ring appearing upfield at about –30 ppm. Ring methyl and methylene proton resonances did not extend further than 28 ppm downfield. When these results are compared with the spectrum of SiR-HP^{1-} (Figures 7, 8B, and 9), it is possible to assign the spectrum of the enzyme to that of a high spin heme with the resonances downfield of 30 ppm arising from meso protons. However, we consider this possibility to be unlikely given the difficulty we have encountered in detecting the broad meso proton resonances in siroheme. In addition, reduction of the cluster in SiR-HP changes the spin state of siroheme to the ferrous high spin form as shown both by resonance Raman and Mossbauer spectroscopies (Han et al., 1989a; Christner et al., 1983a). The NMR spectrum resulting when SiR-HP is reduced from the intermediate to the fully reduced state shows changes which are in accord with those seen for model iron porphyrins on going from $S = 1$ to $S = 2$ ferroheme. Taken together, these data suggest, despite the absence of ferrous isobacteriochlorin model compounds, that in SiR-HP^{1-} siroheme is probably $S = 1$.

Paramagnetic NMR cannot only be used to determine the spin state of the heme, but, in addition, the hyperfine shifts of cysteine resonances allow measurement of spin density on the cluster, which in turn reflects the degree of coupling present between prosthetic groups. The large size of cluster hyperfine shifts, along with the presence of both upfield and downfield shifted resonances, indicate that, for SiR-HP^{1-}, as in the oxidized enzyme, through bond coupling is maintained between the heme and the cluster in solution.

Not only can the presence of coupling be detected, but also the magnitude of the hyperfine shift can be used to estimate the relative size of coupling. Since movement of the cluster cysteines changes the angular terms of the hyperfine shift equation (eq. 3), an assumption must be made regarding motion at the cluster coordinating cysteines upon reduction of the heme. One might well expect there to be motion at the bridging ligand, as change in the spin/oxidation state of the heme iron would be directly sensed by this ligand; however, the other three cysteines might be expected to show much less or even no change in the steric properties of their coordination to cluster irons. Making these assumptions allows one to make direct comparison of the spin densities on the cluster in the $S = 5/2$ ferric form of the enzyme to that in the $S = 1$ ferrous state, since the angular terms in the isotropic shift equations can be set equal to one another. Deuterium labeling of the cysteine residues in the intermediate reduced form of SiR-HP identifies five resonances as arising from the cluster (Figures 7, 8B, and 9; Table IV). A similar pattern of shifts is observed for SiR-HP^{1-}, as compared to the fully oxidized enzyme, with two far downfield shifted resonances, one moderately downfield resonance, and two upfield resonances.[11] The two upfield resonances show a 7% increase in isotropic shift, with loss of degeneracy in intermediate vs resting enzyme, while the two most downfield shifted peaks demonstrate an average shift increase of 14%. Resonance f, tentatively assigned to the bridging cysteine, shows a 47% loss of its isotropic shift. While

[11] The loss of degeneracy may be indicative of a change in the angular terms for the contact shift dependency. With the restraints that the value of $\cos^2 \phi_i$ must be equal and that ϕ_i for two geminal protons differs by 120°, two solutions are possible for identically shifted protons: 60°, –60° or 240°, 120°. A change in the angular terms by only 0.1° can account for the observed 0.2 ppm difference present in SiR-HP^{1-}. Such a small change does not seriously disrupt the assumption that no angular changes occur within the cluster on reduction of the heme. By taking into account this change, a small increase in spin density is still observed.

a change in the angular term ϕ_i could in principle account for this loss, lengthening of the heme Fe–S bond along with decreased heme spin density would also be expected to decrease the magnitude of the observed downfield shift. Taken together, these data suggest that there is either a small increase or no net change of spin density transferred to the cluster upon conversion of resting SiR-HP to the one-electron reduced state. However, the total unpaired spin density available decreases by a factor of 2.5 when $S = 5/2$ is changed to $S = 1$; this means that the heme to cluster coupling must increase by just this amount to keep the spin density on the cluster constant. It can be hypothesized, on the basis of the constancy of spin density transferred from the heme to the cluster, that the protein environment of SiR-HP may well force the cluster into a conformation which is best achieved by a particular net charge on the cluster.

The above results suggest that, in SiR-HP^{1-}, the siroheme moiety is ferrous $S = 1$. In addition, the large size of cluster hyperfine shifts observed requires the existence of a through bond connection between heme and cluster. These results then require the existence of at least a five-coordinate intermediate spin ferrous heme. There are, unfortunately, no satisfactory models for this type of state since all synthetic ferrous intermediate spin hemes reported to date have been on four-coordinate heme models (Medhi et al., 1989).

Two-Electron Reduced SiR-HP. Addition of a second equivalent of electrons to the intermediate form of photoreduced enzyme generates SiR-HP^{2-}. The fully reduced enzyme in the frozen state shows multiple EPR species that can be divided into two classes (Janick & Siegel, 1982). One class of EPR signals ($g = 5$ type) arises from a high $S = 2$ ferrous siroheme antiferromagnetically coupled to the reduced ($S = 1/2$) cluster, while the other ($g = 2.29$ species) may represent intermediate spin ferrous siroheme similarly coupled to the cluster (Christner et al., 1984). However, room temperature RR spectra of SiR-HP^{2-} differed markedly from those exhibited by SiR-HP^{2-} in the frozen state, in that the liquid solution contains only high spin ferrous heme, while the frozen enzyme yields RR spectra suggestive of both high spin and intermediate (or low) spin ferroheme (Han et al., 1989a). The finding of only high spin ferrous heme in solution for SiR-HP^{2-} is readily confirmed by the NMR spectra (Medhi et al., 1989; Goff & La Mar, 1977; Goff et al., 1977) which show no resonances downfield of 20 ppm which are attributable to the heme. Unlike earlier Mossbauer (Christner et al., 1984) and ENDOR (Cline et al., 1986) studies, paramagnetic NMR can directly examine the magnetic interactions in solution.

Fully reduced [4Fe-4S] ferredoxins are reported to possess only downfield shifted resonances (Poe et al., 1970; Packer et al., 1977; Philips et al., 1974); therefore, the presence of upfield shifts observed in cluster protons in SiR-HP^{2-} must be a result of coupling to the heme. The NMR spectra of the fully reduced enzyme contains six peaks with a nominal integrated intensity of seven protons that have been shown by deuterium incorporation to arise from the β-CH_2 group of cluster cysteine resonances. Two peaks are observed upfield at −27.6 and −57.2 ppm while four peaks are shifted downfield at 111.7, 75.8, 55.7, and 45.2 ppm with the last peak having double intensity. The presence of seven β-CH_2 protons means that at least four cysteines are coordinated to the cluster. This implies that a cysteine acts as the bridging ligand.[12]

The previously discussed coupling model used for the more oxidized states of SiR-HP is clearly not valid for SiR-HP^{2-} since the cluster spin is no longer zero. In addition, reduction of a [4Fe-4S] cluster has been shown by numerous probes (Thompson, 1985) to change the conformation of the oxidized cluster, thus invalidating one of the assumptions necessary for comparison, i.e., that the angular dependencies remain constant. A simple model that can be employed for the fully reduced form (Christner et al., 1984) assumes that the siroheme iron and a single iron site of the [4Fe-4S] cluster, designated site A, are chemically linked by a bridging group. The Hamiltonian for the exchange interaction is then

$$\mathbf{H}_{ex} = k_{AH}(\mathbf{S}_A\mathbf{S}_h) \quad (4)$$

where S_A is the local spin of cluster site A. However, within the ground doublet of the [4Fe-4S]$^{1+}$ cluster, this interaction can be reexpressed in terms of the cluster spin:

$$\mathbf{H}_{ex} = J(\mathbf{S}_c\mathbf{S}_h) \quad (5)$$

where $J = k_{AH}F_1$ and F_1 is an equivalence factor that depends on the electronic structure of the iron–sulfur cluster. Mossbauer spectroscopy on the $g = 5$ type species again divided the cluster into two equivalent pairs (Christner et al., 1984), while ENDOR (Cline et al., 1986) observed at least four inequivalent anisotropic couplings. The signs of the coupling constants for the two equivalent iron pairs could not be determined from the Mossbauer data. Since five protons exhibit downfield shifts in the NMR spectrum of SiR-HP^{2-}, this requires at least three cysteines be associated with these shifted resonances. There are at least two possible ways to achieve this distribution of cysteine resonances. The first is that the three nonbridging cysteines show downfield shifts while the upfield peaks represent a geminal pair from the bridging cysteine. We consider this interpretation unlikely, since studies on model ferrous $S = 2$ thiolate complexes (Lukat et al., 1990; Goff et al., 1977) show that the β-CH_2 group of the thiolate ligand is shifted far downfield. A more plausible approach to the above cysteine distribution is analogous to the model proposed for the oxidized cluster where one pair of irons, which includes site A, has positive spin density. While the nonbridging cysteine is shifted upfield, the bridging cysteine resonance is shifted downfield as a result of coordination to the heme. The other pair of irons has negative spin density, yielding downfield-shifted cysteine resonances.

High Spin ($S = 5/2$) Ferric Siroheme. In the model compound Fe(III)–OEiBC, Sullivan et al. (1991) observed the order of decreasing T_1 relaxation times with pyrrole methylene > pyrroline H ~ pyrroline methylene > meso.[4] This pattern of T_1s could then be used to classify a proton as either a pyrrole methylene, pyrroline methylene, pyrroline proton, or meso proton. Examination of the T_1s for siroheme (Table II) shows a much wider dispersion, a result which fails to fit the pattern reported for either five- or six-coordinate Fe(III)–OEiBC. This behavior may be due to the variety of substituents on the siroheme ring (Figure 1) compared to those of Fe(III)–OEiBC.

Comparison of the NMR spectra of siroheme to that of SiR-HP (Figures 3 and 5A) shows two peaks associated with the heme ring protons in the range of 75–150 ppm for SiR-HP, while four peaks are observed in this range for free siroheme. Five-coordinate complexes of free hemes can exist

[12] An alternative hypothesis which cannot be excluded at this time is the presence of multiple enzyme conformers because whether or not the bridging ligand is cysteine, the presence of more than one enzyme conformer allows three cluster cysteines to generate more than six paramagnetically shifted β-CH_2 peaks. As indicated above, there is clear evidence from EPR and resonance Raman data for multiple spin-state conformers in SiR-HP^{2-} in the frozen state. There is no such evidence for multiple conformers of SiR-HP^{2-} in solution (Han et al., 1989a).

in two conformers depending on which face the fifth ligand is bound (Licoccia et al., 1989). The presence of two conformers of siroheme in solution, but only one in the enzyme, could explain the differing number of far-downfield peaks. Another major difference noted between the siroheme and oxidized SiR-HP spectra is the greater shift range of heme resonances in the enzyme spectrum. A greater dispersion of chemical shifts for protein-bound hemes as opposed to free hemes in solution is commonly observed (Satterlee, 1986). Another possibility that must be considered is five- versus six-coordination. For Fe(III)–OEiBC (Sullivan et al., 1991), the five-coordinate complexes had peaks extending only to 70 ppm, while the six-coordinate DMSO complex had peaks as far as 131 ppm downfield. Free siroheme falls in between these extremes with its farthest downfield peak at 94 ppm. The coordination number of siroheme in resting SiR could not be directly determined, utilizing paramagnetic NMR, from the relative hyperfine shifts of meso protons, since no resonances arising from meso protons could be identified. Siroheme resonances in the protein were seen to extend 127 ppm downfield, a result which might suggest greater similarity to six- rather than five-coordinate Fe(III)–OEiBC. While the applicability of the model compound Fe(III)–OEiBC to siroheme is uncertain, other probes in the frozen and crystal states have indicated that the heme lacks any axial ligand other than the bridging ligand (Cline et al., 1985; McRee et al., 1986).

The classical description of the spin delocalization mechanism for $S = 5/2$ iron porphyrins puts predominantly σ spin density at the pyrrole positions of the macrocycles (La Mar & Walker, 1979; Pawlik et al., 1988). Thus, the β-pyrrole protons have isotropic shifts that are downfield of their diamagnetic equivalents. However, π spin density is thought to be large at meso positions and an important if secondary influence on the contact shifts of β-pyrrole protons. The multiplicity of spin delocalization mechanisms from the five iron d orbitals, each with an unpaired spin, have precluded any more detailed analysis of the contact shift pattern, even in idealized 4-fold symmetric hemin. Hence, no attempt at this time is made to extend such an interpretation to the ferric high spin siroheme complex. This is better left to the low spin ferric siroheme complexes, which possess a single spin restricted to π bonding with the macrocycle (J. Kaufman, L. M. Siegel, and L. D. Spicer, manuscript in preparation).

pH Dependence of Resting SiR-HP. Over the pD range studied (6.0–9.9) in this work, the proton resonances showed a variable degree of pD dependency. While most resonances showed small (~1 ppm) shifts, peak h experienced nearly a 10 ppm shift. The observed pD effect can be due to the protonation/deprotonation of either a heme side chain (acetate or propionate), a nearby protein residue, or a heme ligand. SiR-HP has been shown by X-ray crystallography and ENDOR to lack a distal ligand (Cline et al., 1985; McRee et al., 1986). The pD induced binding of a sixth ligand would be expected to perturb the NMR spectra much more than is observed here. The observed shift range for peak h is much larger than that seen in the simple protonation of propionates in hemes (Satterlee, 1986). An exception to this, however, was observed in the case of cytochrome *c'* where 20 and 30 ppm shifts were observed for heme propionate α-CH_2 protons (Banci et al., 1992). The deprotonation of a propionate in this enzyme appears to result in a major rearrangement in terms of the axial/equitorial nature of the α-CH_2 protons with respect to the heme plane, which is reflected in the large shift variation. Cytochrome *c'* was noted to be unique in that it has two Glu residues close to the propionate moiety experiencing such large shifts. A similar charged residue may be present in SiR-HP, causing the large shifts observed for peak h. However, motion of the geminal partner for peak h is not observed, and no NOEs to h are detected at pH 7.7. Resonance Raman experiments on the cyanide adduct of SiR-HP are consistent with H bonding to the distal ligand from a neighboring residue (Han et al., 1989b). The occurrence of an ionizable residue in the vicinity of the substrate binding site may help facilitate cleavage of S–O and N–O bonds during the multielectron reductions of sulfite to sulfide and nitrite to ammonia (Han et al., 1989b; Siegel & Wilkerson, 1989).

Summary. We have demonstrated in the present work that NMR spectroscopy is a useful tool for studying the active center of the hemeprotein subunit of *E. coli* sulfite reductase. Well-resolved spectra can be obtained for all three redox states of the unligated enzyme with assignment of cysteinyl β-CH_2 resonances achieved by deuterium substitution. The oxidized enzyme possesses four cysteines showing hyperfine shifts, one of which has NOEs to the heme ring and has been tentatively assigned to the bridging cysteine. The large size of both upfield and downfield hyperfine shifts observed for the cluster require that exchange coupling between the heme and the cluster be maintained in all three redox states in solution. NMR spectra of the one-electron reduced enzyme in solution are consistent with the presence of intermediate spin $S = 1$ ferrous heme and oxidized [4Fe-4S] cluster. However, the net spin density on the cluster in this enzyme form is the same as in the resting enzyme, despite the lowering of total unpaired spin density, a result which implies that the coupling has *increased* upon reduction (in spite of the fact that intermediate spin ferrous hemes generally have either no or very weakly bound axial ligands!). The fully reduced enzyme is demonstrated to contain an $S = 2$ heme with NMR resonances due to cluster cysteines shifted both upfield and downfield. pD titration of the resting enzyme suggests that an ionizable residue of the protein is located in close proximity to the heme; this residue may very well be of significance in the multiple protonation/deoxygenation steps required in the multielectron reductions of sulfite to sulfide and nitrite to ammonia.

ACKNOWLEDGMENT

We are most grateful to Jer-Yuarn Wu and Dr. Nicholas Kredich for generously providing us with the plasmid containing strains of *S. typhimurium* and *E. coli* used for overproducing SiR and SiR-HP in some of this work. Without these strains, production of enzyme containing deuterium-labeled cysteine would have been much more difficult particularly since cysteine is a potent repressor of production of sulfite reductase in wild-type strains of enterobacteria. We also thank Dr. John Markley and Dr. Gerd La Mar for helpful comments on this manuscript prior to submission. The Duke Magnetic Resonance Spectroscopy Center instrumentation was funded by grants from the National Institute of Health, the National Science Foundation, and the North Carolina Biotechnology Center.

REFERENCES

Banci, L., Bertini, I., Briganti, F., Luchinat, C., Scozzafava, A., & Oliver, M. V. (1991) *Inorg. Chem. 30*, 4517–4524.

Banci, L., Bertini, I., Turano, P., & Vicens, O. M. (1992) *Eur. J. Biochem. 204*, 107–112.

Bertini, I., Briganti, F., Luchinat, C., Scozzafava, A., & Sola, M. (1991) *J. Am. Chem. Soc. 113*, 1237–1245.

Bertini, I., Capozzi, F., Ciurli, S., Luchinat, C., Messori, L., & Piccioli, M. (1992) *J. Am. Chem. Soc. 114*, 3332–3340.
Christner, J. A., Munck, E., Janick, P. A., & Siegel, L. M. (1981) *J. Biol. Chem. 256*, 2098–2101.
Christner, J. A., Janick, P. A., Siegel, L. M., & Munck, E. (1983a) *J. Biol. Chem. 258*, 11157–11164.
Christner, J. A., Munck, E., Janick, P. A., & Siegel, L. M. (1983b) *J. Biol. Chem. 258*, 11147–11156.
Christner, J. A., Munck, E., Kent, T. A., Janick, P. A., Salerno, J. C., & Siegel, L. M. (1984) *J. Am. Chem. Soc. 106*, 6786–6794.
Cline, J. F., Janick, P. A., Siegel, L. M., & Hoffman, B. M. (1985) *Biochemistry 24*, 7942–7947.
Cline, J. F., Janick, P. A., Siegel, L. M., & Hoffman, B. M. (1986) *Biochemistry 25*, 4647–4654.
Cowan, J. A., & Sola, M. (1990) *Inorg. Chem. 29*, 2176–2179.
Dugad, L. B., La Mar, G. N., Banci, L., & Bertini, I. (1990) *Biochemistry 29*, 2263–2271.
Faeder, J. E., Davis, P. S., & Siegel, L. M. (1974) *J. Biol. Chem. 249*, 1599–1699.
Goff, H. M., & La Mar, G. N. (1977) *J. Am. Chem. Soc. 99*, 6599–6606.
Goff, H. M., La Mar, G. N., & Reed, C. A. (1977) *J. Am. Chem. Soc. 99*, 3641–3646.
Han, S., Madden, J. F., Thompson, R. G., Strauss, S. H., Siegel, L. M., & Spiro, T. G. (1989a) *Biochemistry 28*, 5461–5471.
Han, S., Madden, J. F., Siegel, L. M., & Spiro, T. G. (1989b) *Biochemistry 28*, 5477–5485.
Holmes, R. H., Phillips, W. D., Averill, B. A., Mayerle, J. J., & Herskovitz, T. (1979) *J. Am. Chem. Soc. 96*, 2109–2117.
Janick, P. A., & Siegel, L. M. (1982) *Biochemistry 21*, 3538–3547.
Janick, P. A., & Siegel, L. M. (1983) *Biochemistry 22*, 504–515.
Kang, L., LeGall, J., Kowal, A. T., & Johnson, M. K. (1987) *J. Inorg. Biochem. 30*, 273–90.
Kaufman, J., Siegel, L. M., & Spicer, L. D. (1993) in *Techniques in Protein Chemistry IV* (Angeletti, R. H., Ed.) pp 577–584, Academic Press, San Diego.
Keating, K. A., La Mar, G. N., Shiau, F. Y., & Smith, K. M. (1992) *J. Am. Chem. Soc. 114*, 6513–6520.
Kemp, J. D., Atkinson, D. E., Ehret, A., & Lazzarini, R. A. (1963) *J. Biol. Chem. 238*, 3466–3475.
Krishnamoorthi, R., Markley, J. L., Cusanovich, M. A., Przysiecki, C. T., & Meyer, T. E. (1986) *Biochemistry 25*, 60–67.
La Mar, G. N., & Walker, F. A. (1979) in *The Porphyrins* (Dolphin, D., Ed.) Vol. IV, pp 61–157, Academic Press, New York.
Lecomte, J. L., Unger, S. W., & La Mar, G. N. (1991) *J. Magn. Reson. 94*, 112–122.
Licoccia, S., Chatfield, M. J., La Mar, G. N., Smith, K. M., Mansfield, K. E., & Anderson, R. R. (1989) *J. Am. Chem. Soc. 111*, 6087–6093.
Lukat, G. S., & Goff, H. M. (1990) *Biochim. Biophys. Acta 1037*, 351–359 1990.
Madden, J. F., Han, S., Siegel, L. M., & Spiro, T. (1989) *Biochemistry 28*, 5471–5477.
Massey, V., & Hemmerich, P. (1978) *Biochemistry 17*, 9–17.
McRee, D. E., Richardson, J. S., & Siegel, L. M. (1986) *J. Biol. Chem. 261*, 10277–10281.
Medhi, O. K., Mazumdar, S., & Mitra, S. (1989) *Inorg. Chem. 28*, 3243–3248.
Munck, E. (1982) in *Iron–Sulfur Proteins* (Spiro, T. G., Ed.) pp 147–175, John Wiley and Sons, New York.
Murphy, J. M., Siegel, L. M., Kamin, H., & Rosenthal, D. (1973) *J. Biol. Chem. 248*, 2801–2814.
Ostrowski, J., Wu, J., Rueger, D. C., Miller, B. E., Siegel, L. M., & Kredich, N. M. (1989) *J. Biol. Chem. 264*, 15726–15737.
Packer, E. L., Sweeney, W. V., Rabinowitz, J. C., Sternlicht, H., & Shaw, E. N. (1977) *J. Biol. Chem. 252*, 2245–2253.
Pawlik, M. J., Miller, P. K., Sullivan, E. P., Levstik, M. A., Almond, D. A., & Strauss, S. H. (1988) *J. Am. Chem. Soc. 110*, 3007–3012.
Peck, H. D., & Lissolo, T. (1988) *Symp. Soc. Gen. Microbiol. 42*, 99–132.
Phillips, W. D., McDonald, C. C., Stombaugh, N. A., & Orme-Johnson, W. H. (1974) *Proc. Natl. Acad. Sci. U.S.A. 71*, 140–143.
Poe, M., Phillips, D., McDonald, C. C., & Lovenburg, W. (1970) *Proc. Natl. Acad. Sci. U.S.A. 65*, 797–804.
Satterlee, J. D. (1986) *Annu. Rep. NMR Spectrosc. 17*, 79–177.
Scott, I. A., Irwin, A. J., Siegel, L. M., & Shoolery, J. N. (1978) *J. Am. Chem. Soc. 100*, 7987–7994.
Shelnutt, J. A., Dobry, M. M., & Satterlee, J. D. (1984) *J. Phys. Chem. 88*, 4980–4987.
Siegel, L. M., & Davis, P. S. (1974) *J. Biol. Chem. 249*, 1587–1598.
Siegel, L. M., Murphy, M. J., & Kamin, H. (1973) *J. Biol. Chem. 248*, 251–264.
Siegel, L. M., Davis, P. S., & Kamin, H. (1974) *J. Biol. Chem. 249*, 1572–1586.
Siegel, L. M., Murphy, M. J., & Kamin, H. (1978) *Methods Enzymol. 52*, 436–447.
Siegel, L. M., Rueger, D. C., Barber, M. J., Krueger, R. J., & Orme-Johnson, W. H. (1982) *J. Biol. Chem. 257*, 6343–6350.
Siegel, L. M., & Wilkerson, J. (1989) in *Molecular and Genetic Aspects of Nitrate Assimilation* (Wray, J. L., & Kinghorn, J. R., Eds.) pp 263–283, Oxford Science Publications, New York.
Skjeldal, L., Krane, J., & Ljones, T. (1989) *Int. J. Macromol. 11*, 322–325.
Skjeldal, L., Westler, W. M., Oh, B. H., Krezel, A. M., Holden, H. M., Jacobson, B. L., Rayment, I., & Markley, J. L. (1991) *Biochemistry 30*, 7363–7368.
Sola, M., Cowan, J. A., & Gray, H. (1989) *Biochemistry 28*, 5261–5268.
Strauss, S. H., & Pawlick, M. J. (1986) *Inorg. Chem. 25*, 1921–1923.
Strauss, S. H., Silver, M. E., Long, K. M., Thompson, R. G., Hudgens, R. A., Spartalian, K., & Ibers, J. A. (1985) *J. Am. Chem. Soc. 107*, 4207–4215.
Stolzenburg, A. M., Strauss, S. H., & Holm, R. L. (1981) *J. Am. Chem. Soc. 103*, 4763–4878.
Sullivan, E. P., Grantham, J. D., Thomas, C. S., & Strauss, S. H. (1991) *J. Am. Chem. Soc. 113*, 5264–5270.
Tan, J., & Cowan, J. A. (1991) *Biochemistry 30*, 8910–8917.
Thompson, A. J. (1985) in *Metalloproteins* (Harrison, P., Ed.) pp 79–119, Verlag Chemie, Deerfield Beach, FL.
Vogel, H. J., & Bonner, D. M. (1956) *J. Biol. Chem. 218*, 97–106.
White, W. I. (1978) *The Porphyrins* (Dolphin, D., Ed.) Vol. V, pp 303–340, Academic Press, New York.
Wicholas, M., Mustacich, R., & Jayne, D. (1972) *J. Am. Chem. Soc. 94*, 4518–4522.
Wu, J. Y., Siegel, L. M., & Kredich, N. M. (1991) *J. Bacteriol. 173*, 325–333.
Young, L. J., & Siegel, L. M. (1988) *Biochemistry 27*, 4991–4999.